Natural Hazards Research 4 (2024) 148–168

Contents lists available at ScienceDirect

Natural Hazards Research

journal homepage: www.keaipublishing.com/en/journals/natural-hazards-research

Tunnelling-induced ground surface settlement: A comprehensive review with particular attention to artificial intelligence technologies

Gang Niu, Xuzhen He *, Haoding Xu, Shaoheng Dai

School of Civil and Environmental Engineering, University of Technology Sydney, Ultimo, NSW, 2007, Australia

ARTICLE INFO

Keywords:
Tunnelling
Ground surface settlement
Empirical method
Analytical method
Numerical method
Artificial intelligence
Machine learning

ABSTRACT

Shallow tunnels in urban areas are close to adjacent buildings and municipal pipelines. Ground surface settlement (GSS) due to tunnelling can cause damage to those infrastructures surrounded. Many methods have been proposed for evaluating ground settlement induced by tunnelling, including empirical, analytical, numerical and artificial intelligence methods. This paper reviews the proposed methods in detail based on published 677 articles within past ten years. The principles, assumptions and application scope of those methods are summarized and the advantages and limitations of each method are discussed. Since artificial intelligence (AI) become popular in recent few years, the application of AI in the aspect of tunnelling-induced ground deformation is introduced emphatically. Finally, the challenges of ground displacement prediction by machine learning (ML) are clarified and future research directions are suggested.

1. Introduction

The rapid development of urban areas in recent decades contributes to the increasing demand for underground space utilisation. Tunnels have been regarded as effective choice to overcome congestion problems and relieve traffic pressure. Deep tunnels are constructed within stiff rock generally, which means the stratum is relatively stable and settlement of ground is limited. Compared with deep tunnels, tunnels in shallow depths are always surrounded by soft soil practically. In urban areas, the resulted settlement of ground cannot be neglected. In other words, the construction of tunnel in urban regions is more complicated than in less populated areas.

Tunnel excavation disturbs the original stress statement of ground inevitably, as a result, ground settlement is induced (Chen et al., 2019; Kim et al., 2001; Moghaddasi and Noorian-Bidgoli, 2018; Pourtaghi and Lotfollahi-Yaghin, 2012; Zhang et al., 2020). The settlement of ground poses a threat to nearby structures and infrastructures (Chen et al., 2019; Zhang et al., 2020; Hajihassani et al., 2020; Ocak and Seker, 2013; Pourtaghi and Lotfollahi-Yaghin, 2012). To minimize the risk of damage, accurate prediction of maximum GSS is critical to control it within the tolerance (Chen et al., 2019; Ahangari et al., 2015; Darabi et al., 2012; Hasanipanah et al., 2016; Kim et al., 2001; Moghaddasi and Noorian-Bidgoli, 2018; Zhang et al., 2017). In addition, accurate evaluation and management of GSS can help in selecting suitable construction techniques and materials, thereby ensuring the severability of tunnel over its lifespan. Therefore, a comprehensive understanding of ground settlement is integral not only for the engineering design and construction of the tunnel itself but also for the safety of the ground surface structures.

Tunnelling-induced GSS is influenced by three factors mainly, including ground properties, tunnel geometry as well as excavation and support method (Chen et al., 2019; Hasanipanah et al., 2016; Moghaddasi and Noorian-Bidgoli, 2018). Ground properties are the characteristics of soil and rock around tunnel, the parameters depend on the constitutive models used, and particular ones are friction angle, cohesion, unit weight, Poisson's ratio, Young's modulus, etc. Tunnel geometry reflects the shape and location of tunnel, generally including tunnel depth, tunnel diameter, distance between tunnel and nearby structures. Some researchers adopt ground water table in the classification of tunnel geometry as well. For tunnel excavation and support method, already applied approaches include drill-and-blast method with anchor shotcrete support, mechanical excavation method with steel beam support, shield tunnelling method with lining, etc. Tunnel boring machine (TBM) and liner are regarded as common construction approach of tunnels in urban area. There are many parameters of TBM, such as thrust, torque, penetration rate, advance rate, rotation speed, face pressure, pitching angle, grouting pressure, grouting filling volume, specific energy and so on. As a result, choosing appropriate parameters for performing GSS prediction is a challenge.

According to Ocak and Seker (2013), analysis of short-term ground settlement caused by tunnelling is based on the assumption that the soil is in undrained condition. Commonly, it happens within a few weeks after excavation. For long-term settlement, which is due to creep, stress

* Corresponding author.
E-mail addresses: Gang.Niu@student.uts.edu.au (G. Niu), Xuzhen.He@uts.edu.au (X. He), Haoding.Xu@alumni.uts.edu.au (H. Xu), Shaoheng.Dai@student.uts.edu.au (S. Dai).

https://doi.org/10.1016/j.nhres.2023.11.002
Received 27 September 2023; Received in revised form 29 October 2023; Accepted 3 November 2023
Available online 13 November 2023

redistribution and consolidation of soil, it may take several months to a few years to reach a stabilized stage (Ocak and Seker, 2013). In general, short-term GSS is contributed by construction methods mainly while long-term GSS depends on soil features and tunnel geometry.

This paper initially provides an extensive review of diverse methods proposed for evaluating GSS. Special attention is then paid to investigate the application of ML techniques in GSS prediction. Finally, a comprehensive discussion is concluded and future research directions in the field of GSS prediction through machine learning (ML) are suggested.

2. Overview of traditional methods for ground surface settlement prediction

The study of tunnelling-induced ground surface settlement (GSS) holds a critical place in the field of tunnel research. There are two modulus of ground surface deformation - transverse settlement and longitudinal settlement (shown in Fig. 1). A significant research portion is predicting maximum GSS, which is important for ensuring structural stability and minimizing risks to adjacent buildings and infrastructure. Various methodologies have been proposed to accurately predict and manage maximum GSS, including empirical, analytical, numerical and artificial intelligence methods (Moghaddasi and Noorian-Bidgoli, 2018; Zhang et al., 2017).

Traditional approaches often rely on empirical or analytical equations, which are developed through engineering experience and theorical assumptions. While these methods offer the benefit of simplicity, they are limited in their applicability due to the inherent complexity of geological characteristics. Numerical simulations such as Finite Element Method (FEM) and Finite Difference Method (FDM) provide a more sophisticated approach. These simulation techniques can accommodate a wide array of soil parameters and capture the complex interaction between soil layers and tunnel walls. Over the past few years, the rise of AI and ML techniques had provided a new way for GSS prediction. These AI methods can consider a broader set of variables and offer the advantage of adaptability, learning from newly acquired data to refine future predictions. Beyond the focus on GSS prediction, there is also a growing recognition of the importance of predicting other aspects of ground behaviour, such as time-dependent ground deformation and stress distribution. Spatial-temporal analyses are also becoming increasingly important for real-time monitoring and management of tunnelling-induced GSS.

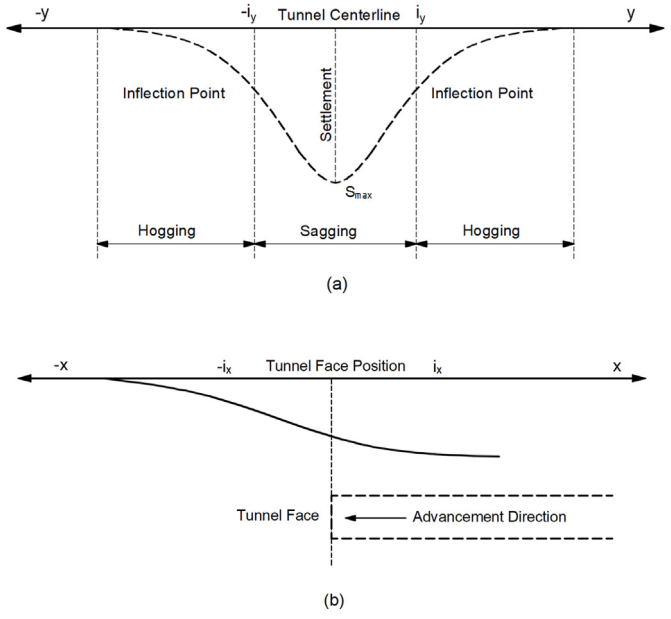

Fig. 1. Tunnelling-induced ground deformation model. (a) transverse settlement trough and (b) longitudinal settlement trough.

2.1. Empirical methods

Empirical methods for evaluating GSS caused by tunnelling are according to engineering practice and measured field data mostly. They provide a roughly estimation of ground subsidence with allowable precision. In other words, empirical methods are proposed simple mathematical equations based on measurements gathered from the field. These formulas can approximately find settlement trough and calculate displacement of ground at any point of the specific region.

Martos (1958) originally proposed that the normal distribution curve can well represent the shape of daily settlement trough. As shown in Fig. 1, Peck (1969) expanded the research and demonstrated that a Gaussian curve was appropriate for fitting tunnelling-induced ground settlement. He analysed the settlement data from many tunnels as well as mines projects and found that the settlement curve was roughly symmetrical above the vertical axis of the tunnel. Subsequently, he offered the equations for estimating GSS, as shown in Equation (1).

$$S_v = S_{max} \exp\left(\frac{-Y^2}{2i^2}\right)$$

$$S_{max} = \frac{V_s}{2.5{*}i}$$

$$V_s = V_L\left(\pi D^2/4\right) \tag{1}$$

Where S_v is the vertical surface settlement at the Y distance from tunnel centreline, S_{max} is the maximum ground surface settlement that usually occurs above tunnel centreline, i is horizontal distance from tunnel centre to point of inflexion of the settlement trough (see Fig. 1), V_s is the settlement volume per unit advancement, V_L is tunnel volume loss, and D is tunnel diameter.

Based on the hypothesis presented by Peck (1969), different methods for calculating the value of S_{max} were investigated. For example, Ranken (1987) optimised the relationship between S_{max} and V_s, as shown in Equation (2). Attewell et al. (1986) proposed a new formula to calculate maximum GSS (Equation (3)). More empirical equations are summarized in Table 1. In addition, the inflection point (i), which determines the shape of settlement trough, may vary in different ground conditions. It is also dependent on tunnel depth and tunnel radius significantly. The empirical equations for estimating inflection point (i) are shown in Table 2.

$$S_v = S_{max} \exp\left(\frac{-X^2}{2i^2}\right)$$

$$S_{max} = \frac{V_s}{i\sqrt{2\pi}} \tag{2}$$

$$S_{max} = \frac{(1+\mu^2)P_v}{E}\frac{4HR^2}{H^2-R^2} \tag{3}$$

Where S_{max} is the maximum ground surface settlement, S_v is the vertical surface settlement at the X distance from tunnel centreline, V_s is the settlement volume per unit advancement, H is tunnel depth and R is tunnel radius, X is horizontal distance between pile and tunnel centreline, P_v is vertical component of the principal in situ stress, E is elastic modulus, μ is Poisson's ratio.

Empirical equations have long been a convenient and straightforward methodology for estimating GSS caused by tunnel construction. Those formulas are summarized and developed based on engineering experiences and field observation, taking the assumptions that soil properties are uniform across tunnel alignment, tunnelling methods applied in new project is similar to those of previous projects, 3D effects can be ignored, ground conditions are similar, and so on. Empirical formulas are not applicable in all projects (Chen et al., 2019), they are mostly suitable for soft ground condition. For different strata conditions, the parameters

Table 1
Empirical formulas for predicting tunnelling-induced ground settlement.

Empirical Formula	Application Conditions	Reference
$S_{max} = 0.0125\frac{V_L}{i}\times\left(\frac{D}{2}\right)^2$	clay and sand	Schmidt (1969)
$S_{max} = f\left(\frac{H}{2R}\right)$	clay	Attewell and Farmer (1974)
$S_{max} = \frac{V_s}{\sqrt{2\pi}\times i}$	clay and sand	Yoshikoshi et al. (1978)
$S_{max} = \frac{V_s}{\sqrt{2\pi}i}\left[G\left(\frac{x-x_i}{i}\right) - G\left(\frac{x-x_f}{i}\right)\right]$	clay and sand	Attewell and P Woodman (1982)
$S_{max} = 0.785[\gamma_n \times H + \sigma_s]\times\frac{D^2}{i\times E}$	clay and sand	Herzog (1985)
$S_{max} = 4.71[\gamma_n \times H + \sigma_s]\times\frac{D^2}{(3i+d)\times E}$	twin tunnels in clay and sand	Herzog (1985)
$S_{max} = \frac{V_L}{\sqrt{2\pi}k(H-h)}\exp\left[-\left(\frac{x}{\sqrt{2\pi}k(H-h)}\right)^2\right]\ k = \frac{0.175+0.325(1-h/H)}{1-h/H}$	clay	Mair et al. (1993)
$S_{max} = 0.313\left(\frac{V_L\times D^2}{i}\right)$	clay and sand	Mair and Taylor (1997)
$S_{max} = 4.71[1-0.71\times\exp(-0.018\times d)]\times(\gamma_n\times H+\sigma_s)\times\frac{D^2}{(3i+d)\times E}$	clay and sand	Hasanpour et al. (2012)
$S_{max} = 0.01875\left(\frac{D^2}{4i}\right)\times e^{0.26[\gamma_n\times H+\sigma_s-\sigma_T]/Cu}$	clay and sand	Chakeri et al. (2013)
$S_{max} = \frac{V_L(1.82-(H-h)/H)}{1.85\times\sqrt{2\pi}k(H-h)}\exp\left[-\left(\frac{x}{\sqrt{2k}(H-h)}\right)^2\right]\ k = -\frac{2.8(H-h)}{H}+2.1$	sand	Wang et al. (2016)
$S_{max} = \frac{V_L(\frac{0.5h}{H}+0.5)}{\sqrt{2\pi}k(H-h)}\exp\left[-\left(\frac{x}{\sqrt{2\pi}k(H-h)}\right)^2\right]\ k = \frac{0.44-(0.28h/H)}{1-h/H}$	sand	Wang (2021)

Table 2
Empirical formulas for the calculation of inflection point.

Settlement Trough (i)	Application Conditions	Reference
$i = H/\left[\sqrt{2\pi}\times\tan\left(\frac{\pi}{4}-\frac{\varphi}{2}\right)\right]$	clay and sand	Peck (1969)
$i = 0.4H + 1.92$	clay and sand	Schmidt (1969)
$i = 0.5H$	clay	Glossop (1978)
$i = R\left(\frac{H}{D}\right)^{0.8}$	clay and sand	Clough and Schmidt (1981)
$i = K\times H$	K= 0.2 – 0.3 for sand K= 0.4 – 0.7 for clay	O'Reilly and New (1982)
$i = 0.43H + 1.1$	clay	
$i = 0.4H + 0.6$	clay	Herzog (1985)
$i = 0.9\left(\frac{D}{2}\right)\times\left(\frac{H}{D}\right)^{0.88}$	clay and sand	Arioglu (1992)
$i = 0.386H + 2.84$	clay and sand	
$i = 1.392\left(\frac{D}{2}\right)\times\left(\frac{H}{D}\right)^{0.704}$	clay	
$i = \frac{D}{2}\times 1.15\left(\frac{H}{D}\right)^{0.9}$	clay	Loganathan and Poulos (1998)
$i = \frac{H}{D}$	clay and sand	Hamza et al. (1999)
$i = \frac{D}{2}\times\left(\frac{H}{D}\right)^{0.8}$	clay	
$i = 0.74\left(\frac{D}{2}\right)\times\left(\frac{H}{D}\right)^{0.9}$	sand	
$i = 0.63\left(\frac{D}{2}\right)\times\left(\frac{H}{D}\right)^{0.97}$	sand	
$i = 0.29H + R$	clay	Lee (1999)
$i = \frac{1}{3}\left(0.886H + 0.696D\times\left(\frac{H}{D}\right)^{0.704} + 2.84\right)$	clay	Ercelebi et al. (2005)
$i = \frac{1}{4}[0.93H + R\times(0.9\left(\frac{H}{D}\right)^{0.88} + \left(\frac{H}{D}\right)^{0.8}) + 1.1]$	clay and sand	Ercelebi et al. (2011)
$i = \frac{1}{7}[2.116H + R\times(0.9\left(\frac{H}{D}\right)^{0.88} + \left(\frac{H}{D}\right)^{0.8}) + 6.46]$	sand	Chakeri et al. (2013)
$i = 0.56309\times H - 0.40978\times D$	sandy cobble strata	Wang et al. (2023)

i is inflection point, R is tunnel radius, D is tunnel diameter, H is tunnel depth. φ is friction angle of soil.

selection of the empirical formula varies greatly (Su et al., 2022). Moreover, empirical methods often suffer from a lack of comprehensive soil parameter inclusion, which means the accuracy of the GSS prediction based on the empirical method cannot be guaranteed (Zhang et al., 2017). The limited number of settlement markers available in site also restricts the accuracy of empirical methods. According to Zhang et al. (2020), the variability of predicted results using empirical methods tend to be large. Considering these constraints and limitations, while empirical methods will continue to be a tool for tunnel construction planning, they should be used in conjunction with other more advanced and

comprehensive methodologies such as numerical simulations or machine learning (ML) algorithms, for more reliable and accurate GSS prediction.

S_{max} is the maximum ground surface settlement that usually occurs above tunnel's centreline, V_s is the settlement volume per unit advancement and V_L is tunnel volume loss, i is horizontal distance from tunnel centre to point of inflexion of the settlement trough while R and D are tunnel radius and tunnel diameter respectively. It needs notice that h and H are depth of the calculated settlement trough from the ground surface and tunnel depth respectively. d is distance between tunnel axes, E is elastic modulus, γ_n is natural unit weight of soil, C_u is undrained cohesion, k is empirical constant of proportionality, σ_s is surface surcharge, σ_T is required face support pressure, x is the longitudinal position of the considered surface point, x_i is the initial position of the tunnel, x_f is the location of the tunnel face, and G is the numerical integration of the normal probability curve. When $x = x_f$, the quantity of G is 0.5, and when $(x - x_i)$ approaches infinity, the quantity of G approaches one. This part is the illustration of each sign in Table 1, thus it should be located at the bottom of Table 1.

2.2. Analytical methods

Analytical methods take into account more influential factors and simulate ground responses in a simple manner. They are developed based on fundamental equations of elastic theory. Multiple analytical approaches such as mirror image method, stress function method, complex variable function method, random medium theory and energy conservation method have been proposed to theoretically analyse GSS caused by tunnel construction. The special attention is devoted to analysing the interactions between ground and tunnel.

Sagaseta (1987) presented an approach for determining near-ground-surface stress and strain field induced by point sink. Based on the assumption that soil material is homogeneous and incompressible, he developed the parameter of ground loss (ε) to predict surface subsidence ($z = 0$) during tunnel excavation. The formulas are shown in Equation (4)

$$S_x = -\frac{\varepsilon}{2\pi}\frac{x}{x^2+H^2}\left(1+\frac{y}{(x^2+y^2+H^2)^{0.5}}\right)$$
$$S_y = \frac{\varepsilon}{2\pi}\frac{1}{(x^2+y^2+H^2)^{0.5}} \tag{4}$$
$$S_z = \frac{\varepsilon}{2\pi}\frac{H}{x^2+H^2}\left(1+\frac{y}{(x^2+y^2+H^2)^{0.5}}\right).$$

Where H is tunnel depth, ε is ground loss, x and y are coordinates at ground surface, which physically means x is horizontal distance from tunnel centreline and y is the distance from tunnel face.

Verruijt and Booker (1996) investigated GSS due to tunnel deformation by employing elastic half plane theory. They set up two tunnel deformation mechanisms including a uniform radial displacement (shown in Fig. 2) and an ovalisation of tunnel. Assuming soil is elastic material, they proposed analytical expressions for calculating the displacements at any points of the half plane. The formulas for calculating vertical and lateral displacement of arbitrary positions are shown in Equation (5). Later, Loganathan and Poulos (1998) modified the approach above and introduced new ground loss parameter that incorporates nonlinear ground movement around tunnel-soil interface (see Fig. 2). With short term consideration only, they neglect the ground deformation due to tunnel ovalisation ($\delta = 0$). In this case, the analytical method proposed by Loganathan and Poulos (1998) is suitable for clay in undrained situation merely. The optimised formulars are expressed in Equation (6).

$$U_z = -\varepsilon R^2\left(\frac{z_1}{r_1^2}+\frac{z_2}{r_2^2}\right)+\delta R^2\left[\frac{z_1(kx^2-z_1^2)}{r_1^4}+\frac{z_2(kx^2-z_2^2)}{r_2^4}\right]+\frac{2\varepsilon R^2}{m}\left[\frac{z_2(m+1)}{r_2^2}-\frac{mz(x^2-z_2^2)}{r_2^4}\right]-2\delta R^2 H\left[\frac{x^2-z_2^2}{r_2^4}+\frac{m}{m+1}\frac{2zz_2(3x^2-z_2^2)}{r_2^6}\right]$$
$$U_x = -\varepsilon R^2\left(\frac{x}{r_1^2}+\frac{x}{r_2^2}\right)+\delta R^2\left[\frac{x(x^2-kz_1^2)}{r_1^4}+\frac{x(x^2-kz_2^2)}{r_2^4}\right]-\frac{2\varepsilon R^2 x}{m}\left[\frac{1}{r_2^2}-\frac{2mzz_2}{r_2^4}\right]-\frac{4\delta R^2 xH}{m+1}\left[\frac{z_2}{r_2^4}+\frac{zm(x^2-3z_2^2)}{r_2^6}\right] \tag{5}$$

$$U_{z=0} = 4(1-\mu)R^2\frac{H}{H^2+x^2}\frac{4gR+g^2}{R^2}\exp\left[-\frac{1.38x^2}{(H+R)^2}\right]$$
$$U_x = -xR^2\left[\frac{1}{x^2+(H-z)^2}+\frac{3-4\mu}{x^2+(H+z)^2}-\frac{4z(z+H)}{\left(x^2+(H+z)^2\right)^2}\right]\times\frac{4gR+g^2}{4R^2}\exp\left\{-\left[\frac{1.38x^2}{(H+R)^2}+\frac{0.69z^2}{H^2}\right]\right\} \tag{6}$$

Where ε is uniform radial ground loss, δ is long-term ground deformation due to ovalisation of tunnel, g is gap parameter, $z_1 = z - H$ and $z_2 = z + H$, $r_1^2 = x^2 + z_1^2$ and $r_2^2 = x^2 + z_2^2$, R is tunnel radius and H is tunnel depth, $m = 1/(1-2\mu)$, $k = \mu(1-\mu)$, μ is soil Poisson's ratio.

Similarly, Gonzaíez and Sagaseta (2001) improved the mentioned analytical equations by considering soil volumetric compressibility. They clarified that the total deformation of tunnel is caused by three parts: ground loss, ovalisation and vertical movement of tunnel itself (depicted in Fig. 3). The general equations for analysing ground movement at surface are shown in Equation (7). The results are compared with actual measurements and show a good agreement. It means the proposed formulas can reflect soil deformation patterns in various situations with reasonable accuracy and can be employed in a wide range of cases (Gonzaíez and Sagaseta, 2001).

$$S_{z=0} = 2\varepsilon R\left(\frac{R}{H}\right)^{2\alpha-1}\times\frac{1}{(1+x'^2)^{\alpha}}\left(1+\rho\frac{1-x'^2}{1+x'^2}\right)$$
$$S_x = -2\varepsilon R\left(\frac{R}{H}\right)^{2\alpha-1}\times\frac{x'}{(1+x'^2)^{\alpha}}\left(1+\rho\frac{1-x'^2}{1+x'^2}\right) \tag{7}$$

Where H is tunnel depth, R is tunnel radius, u is uniform radial displacement, α is exponent for volumetric compressibility, ε is radial contraction (u/R), δ represents ovalisation, ρ is relative ovalisation (δ/ε), the prime ($'$) means the magnitudes are scales by tunnel depth.

Antonio Bobet (2001) discussed different construction processes and soil conditions, including shallow tunnel in dry ground, shallow tunnel in saturated ground and shallow tunnel in saturated ground with air pressure. For the last two cases, long-term and short-term analysis are conducted. The liner is assumed to be incompressible and flexible, while both ground and liner behave elastically. According to analytical analysis, he concluded: (1) The presence of water table decreases settlement at ground surface. (2) The dissipation of pore pressure causes an increase

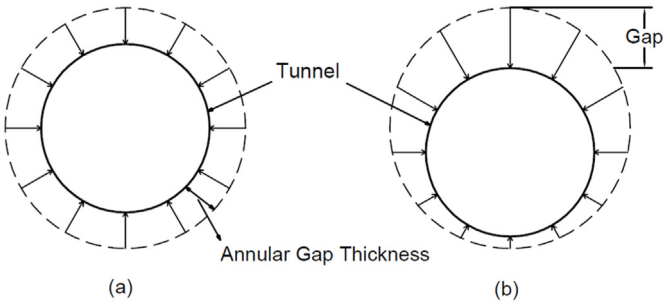

Fig. 2. Circular ground deformation patterns around tunnel section. (a) Uniform contraction (Verruijt and Booker, 1996) and (b) Uniform contraction with vertical displacement (Loganathan and Poulos, 1998).

in ground deformations. (3) Most of ground deformations happen during the undrained phase of tunnel construction. (4) Excavation with air pressure produces larger settlement than that of without air pressure. The details are shown in Equation (8)(9)(10)(11)(12). Further, following the outcome illustrated by Antonio Bobet (2001), Chou and Bobet (2002) analysed the condition that water table is at the ground surface. They compared the analytical results with field observations where tunnels are constructed within soft to stiff clay below water table. The analytical solution gives reasonable prediction for shield driven tunnels in medium to stiff clay (Chou and Bobet, 2002). In addition, it is explained that during excavation of tunnel, the internal air pressure is commonly applied to prevent water inflow into the tunnel (Antonio Bobet, 2001). The value of air pressure is taken as the magnitude of the water pressure at invert of tunnel (Antonio Bobet, 2001; Chou and Bobet, 2002).

In dry ground,

$$S_{\max}=-\frac{gR}{H}+\frac{1+\mu}{E}\left\{\gamma R^2\left[\frac{1}{8}\left(k-\frac{\mu}{1-\mu}\right)\left(\frac{R}{H}\right)^2-\frac{1}{4}\frac{3-4\mu}{1-\mu}\ln H\right]+\gamma H(1-k)R\left[-2(1-\mu)\frac{R}{H}+\frac{1}{8}(9-4\mu)\left(\frac{R}{H}\right)^3-\frac{1}{4}\left(\frac{R}{H}\right)^5\right]\right\} \tag{8}$$

In saturated ground, short-term analysis,

$$S_{\max}=-\frac{gR}{H}+\frac{1+\mu}{E}\left\{-\frac{1}{2}\gamma R^2\ln H+\gamma_b H(1-k)R\cdot\left[-\frac{R}{H}+\frac{3}{4}\left(\frac{R}{H}\right)^3-\frac{1}{4}\left(\frac{R}{H}\right)^5\right]\right\} \tag{9}$$

In saturated ground, long-term analysis,

$$S_{\max}=-\frac{gR}{H}+\frac{1+\mu}{E}\left\{\gamma R^2\left[\frac{1}{8}\left(k-\frac{\mu}{1-\mu}\right)\left(\frac{R}{H}\right)^2-\frac{1}{4}\frac{3-4\mu}{1-\mu}\ln H\right]+\frac{1}{8}\gamma_w(1-k)\frac{R^4}{H^2}+\gamma_b H(1-k)R\cdot\left[-2(1-\mu)\frac{R}{H}+\frac{1}{8}(9-4\mu)\left(\frac{R}{H}\right)^3-\frac{1}{4}\left(\frac{R}{H}\right)^5\right]\right\} \tag{10}$$

In saturated ground with air pressure, short-term analysis,

$$S_{\max}=-\frac{gR}{H}+\frac{1+\mu}{E}\left\{-\frac{1}{2}\left[\gamma R^2\ln H+\gamma_b H(3-k)R^2\right]+\gamma_b H(1-k)R\left[\frac{3}{4}\left(\frac{R}{H}\right)^3-\frac{1}{4}\left(\frac{R}{H}\right)^5\right]+\gamma_w HR\left(\frac{R}{H}\right)^2\right\} \tag{11}$$

In saturated ground with air pressure, long-term analysis,

$$S_{\max}=-\frac{gR}{H}+\frac{1+\mu}{E}\left\{-\frac{1}{2}\left[\frac{3-4\mu}{2(1-\mu)}\gamma R^2\ln H+\gamma_b(1+k)R^2\right]+\frac{1}{8}\frac{1-2\mu}{1-\mu}\gamma HR\left(\frac{R}{H}\right)^3+\gamma_b H(1-k)R\left[-2(1-\mu)\frac{R}{H}+\frac{2-\mu}{2}\left(\frac{R}{H}\right)^3-\frac{1}{4}\left(\frac{R}{H}\right)^5\right]+\gamma_w HR\left(\frac{R}{H}\right)^2\right\} \tag{12}$$

Where E is Young's modulus of soil, μ is Poisson's ratio, H is tunnel depth, R is tunnel radius, g is gap between ground and liner, γ is total unit weight of ground, γ_w is unit weight of water, γ_b is buoyant unit weight of ground, k is coefficient of earth pressure at rest, $S_{\max}$ is maximum surface settlement above tunnel centreline.

Park (2004) optimised the analytical method through employing correction factors. By imposing the oval-shaped ground determination pattern as boundary condition around tunnel section, Park (2004) considers a real nonuniform ground deformation pattern. The analysis model is based on the assumption that soil is elastically incompressible with short-term undrained ground conditions ($k=1$ *and* $\mu=0.5$). Detailed formulas are shown in Equation (13).

$$\begin{aligned}u_z&=-\frac{1.5}{E_u}\left[\frac{a_0}{r}\sin\theta+\frac{\gamma R^2}{2}\left\{\ln r\left(\sin^2\theta-\cos^2\theta\right)-\cos^2\theta\right\}\right]\\ u_x&=-\frac{1.5}{E_u}\left[\frac{a_0}{r}\cos\theta-\frac{\gamma R^2}{2}\cos\theta\sin\theta\right]\end{aligned} \tag{13}$$

Where E_u is undrained Young's modulus of soil, γ is unit weight of ground, a_0 is determined from boundary condition, R is tunnel radius, r and θ are polar coordinates.

More analytical methods for solving ground surface settlement (GSS) problem can refer to New and O'Reilly (1991), Chi et al. (2001), Chakeri and Ünver (2014), Fang et al. (2017), Yuan et al. (2018), Zhang et al. (2020), Franza and Marshall (2019), Fang et al. (2023) and so on.

From discussed above, the summary can be drawn. Analytical solution is accepted in many applications as it provides solution for the case of ground loss for the incompressible soil (Zhang et al., 2017). But it tends to underestimate the maximum soil deformation or overestimate the settlement trough since time-dependent consolidation and creep of ground are ignored (Chen et al., 2019; Zhang et al., 2017). Meanwhile, analytical solution adopts many assumptions, for example, the soil material is elastic, homogeneous and incompressible. Since GSS is a nonlinear problem with high dimensional inputs, it is hard to model

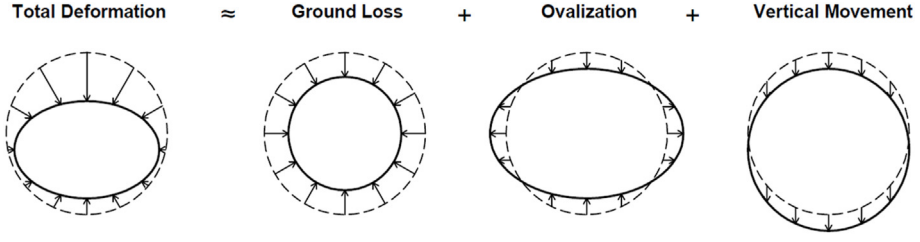

Fig. 3. Components of tunnel deformation illustrated by Gonzaíez and Sagaseta (2001).

soil-tunnel interaction by analytical methods. Su et al. (2022) also indicated that analytical methods are difficult to describe the complex nonlinear relationship between tunnel and the ground settlement due to its relatively simply form and limited influencing factors. The results obtained from analytical theories cannot be guaranteed. Thus, it is suggested that analytical solution is applicable to short-term undrained conditions but fails to be employed when the ground deformation around tunnel section is small such as rock (Zhang et al., 2017).

2.3. Numerical methods

In response to the increasing computing capability, numerical methods have been accepted as effective tool for tunnel analysis in complex geometrical conditions. Numerical approaches can overcome some limitations of empirical and analytical methods. For example, it allows more input parameters that have influence on the settlement of ground surface to be considered. Finite element method (FEM) and finite difference method (FDM) are two widespread numerical methods in tunnel analysis. Both have been employed to analyse various problems with tunnels such as tunnel convergence, leakage of tunnel, tunnel excavation process, tunnel stability and ground subsidence caused by tunnelling. For example, Zhao et al. (2017) and Huang et al. (2015) employed FEM to investigate tunnel convergence, while Huang et al. (2017), Zhang et al. (2021) took advantage of FDM to study tunnel deformation in spatially variable soil. The simulation of tunnel excavation process is conducted by many researchers such as Kasper and Meschke (2004), Kasper and Meschke (2006a), Kasper and Meschke (2006b) and Xie et al. (2016). On other aspects, Zhang et al. (2021) predicted excavation disturbed zone by FEM. They used a linear elastic constitutive model to describe the mechanical behaviour of rock, while the mechanical properties of soil were modelled by Mohr-Coulomb elastic-perfectly plastic constitutive model. Outcomes show that rock content, rock size, rock strength and lateral pressure coefficient influence the disturbed zone significantly while tunnel radius and tunnel depth have small effects.

In terms of GSS due to tunnelling, proposed numerical simulation methods are gap method, stress reduction method, stiffness reduction method, contraction method, grouting pressure method and step-by-step method mainly. The main publications in 2021 and 2022 are summarized in Table 3. As can be revealed, the original study primarily concentrates on two-dimensional (2D) analyses, overlooking the spatiotemporal effects associated with tunnelling. It simulates a solitary step without taking the whole tunnelling procedure into account. For instance, the stress reduction method is implemented by creating a tunnel that is initially in equilibrium with the pressure from the surrounding soil mass. Subsequently, the support pressure is progressively diminished to mimic the tunnel excavation process. However, this approach neglects crucial aspects such as the grouting process and face balance of TBM which can be simulated within a three-dimensional (3D) framework.

Recently, the most popular employed simulation method is full excavation process method (step-by-step method). A systematic process for tunnel construction simulation can be briefly outlined as follows: (1) Establish the initial ground condition and balance the geostatic stresses. (2) Apply face pressure at the tunnel face and supporting pressure along the tunnel outline. (3) Simulate TBM excavation by gradually deactivating soil elements inside the tunnel until all soil elements are excavated. (4) Install liner by activating predesigned lining elements. Concurrently, variations in face pressure can be employed to model the stoppage of TBM. (5) Activating grouting pressure. (6) Optionally, the hardening process of the grouting material and the weight of the grout filling can be simulated in the end. These processes are repeated until the whole tunnel is constructed. This step-by-step analysis approach permits soil to undergo vertical displacement freely under the influence of gravity during tunnelling. The commonly applied constitutive model of soil is linear elastic with Mohr–Coulomb failure criterion, followed by Cam-Clay model. When considering time factor, viscous, consolidation and creep constitutive model of soil should be applied. Underground support structures such as liner are always assumed to exhibit elastic behaviour due to the significantly higher relative strength and Young's modulus of concrete compared to soil. The elastic deformation of liner caused by the overburden pressure of soil makes a limited contribution to GSS, thus rendering it negligible.

The interactions between tunnel and surrounding structures (building, pile, tunnel, excavation) are investigated further. Potts (1997) analysed the interaction between building and tunnelling by parametric study. Mroueh and Shahrour (2003) employed a 3D finite element model to analyse the tunnelling–adjacent structures interaction. They assumed soil is elastic Mohr–Coulomb plastic material, the behaviour of nearby building during tunnel construction was presented. Houhou et al. (2022) analysed the behaviour of single pile and pile group due to tunnelling-induced ground movement. It is reported that the results obtained from 2D finite element simulation tends to be conservative, which means the responses of pile is overestimated (Houhou et al., 2022). Compared with 3D analysis, applying 2D simulation can simplify constitutive model and save calculation time. However, 2D analysis requires to consider 3D tunnelling effect as a result of volume loss (Karakus, 2007). In instances where multiple tunnels are being constructed adjacently, analysis of GSS caused by a single tunnel is insufficient. Hage Chehade and Shahrour (2008) studied the influences of relative position and construction procedure of twin tunnels on GSS using FEM. Based on modified Cam-Clay soil and elastic liner assumption, Zheng et al. (2022) also employed FEM to investigate the interaction of overlapping tunnels. More complex situation was investigated by Chakeri et al. (2011). Stress distribution, deformations and surface settlements were simulated in the condition of two tunnels pass beneath one tunnel. Under intricate environmental circumstances, (such as multiple adjacent tunnels), empirical and analytical solutions often falter in accurately predicting GSS. In contrast, numerical simulation is a highly suitable method for such analyses. However, the efficacy of numerical simulations heavily depends on the constitutive models adopted.

In summary, numerical method is widely used in geotechnical engineering. It is a theoretically more realistic and rigorous method for estimating GSS (Zhang et al., 2020). With the ability to consider various relevant factors, such as nonlinear behaviour of soil, ground heterogeneity, underground water level and soil-tunnel interaction, numerical method is proved to be an effective approach for tunnel analysis. However, numerical method is criticised by its efficiency as simulation models are time-costing and sensitive to boundary condition (Zhang et al., 2017). The accuracy of numerical methods depends on the size of mesh and the selection of failure criterion model. Geotechnical materials often exhibit nonlinear, inelastic, and time-dependent characteristics. Although many advanced numerical methods attempt to simulate these complex properties, fully simulating real-world situations remains a challenge. Identifying the relevant elements to introduce into numerical model is another main factor influencing simulation accuracy. The determination of some parameters of constitutive model may relies on laboratory experiments (Chen et al., 2019). Additionally, the excavation process is difficult to simulate, and the obtained results sometimes differ from field measurement and case histories (Pourtaghi and Lotfollahi-Yaghin, 2012).

3. Overview of artificial intelligence methods

Currently, using computer technology to establish prediction models is a research focus. ML performs well in solving complex mapping problems and becomes popular in engineering field. The wide application of ML in geotechnical engineering provides a new option for analysing soil and rock behaviours dynamically. Compared with the traditional empirical formulas and theoretical analysis methods, AI method can implement many functions with higher accuracy. Those AI methods, such as Artificial Neural Network (ANN), Decision Tree (DT), Radom Forest (RF), Support Vector Machine (SVM), Convolutional Neural Network (CNN), Recurrent Neural Network (RNN), and K-Nearest Neighbors (KNN), have been successfully employed in tunnel

Table 3
Analysis of tunnelling-induced ground deformation by numerical method between 2021 and 2022.

Simulation Method/Boundary Condition	Dimension	Constitutive Model		References	Studied Problems
		Soil	Liner		
Gap Method	2D	Cam-Clay and MC	Elastic	Mansour et al. (2021)	GSS in Port-Said clay considering effects of grouting pressure and consolidation
Contraction Method	2D	MC	Elastic	Saeed and Uygar (2022)	The effect of tunnel geometry and volume loss on the maximum GSS.
				Topal and Mahmutoğlu (2021)	Analysis of GSS induced by tunnelling for Esenler-Basaksehir subway line
Stress Reduction Method	2D	Cam-Clay	Elastic	Tian et al. (2022)	GSS due to tunnelling in anisotropic ground
		MC	Elastic	Mojtahedi and Nabizadeh (2022)	GSS due to twin-tunnel excavation
Stiffness Reduction Method	3D	Cam-Clay	Elastic	Hu et al. (2022)	The effect of construction sequence on GSS in case of triple stacked tunnelling
Full Tunnelling Process Simulation (step-by-step method)	3D	MC	Elastic	He et al. (2021)	GSS due to tunnelling in sandy cobble strata
				Zhong et al. (2021)	GSS induced by twin tunnels construction in soil-rock mixed ground
				Ahmed et al. (2021)	GSS due to tunnelling under existing tunnel
				Li et al. (2021)	GSS induced by curved shield tunnelling
				Chakeri et al. (2021)	Influence of annular gap on GSS
				Dehghan et al. (2021)	Influence of face pressure and grouting pressure on GSS
				Ke et al. (2021)	Interaction between mechanically driven tunnel construction and surrounding soil
				Li et al. (2021)	Influence of asymmetric tunnelling construction scheme on GSS
				Do Ngoc et al. (2022)	GSS induced by twin tunnels construction
				Zhang et al. (2022)	The effect of grout material properties on GSS, i.e. immediately solidified, quick hardening and good mobility type.
				Deng et al. (2022)	GSS caused by tunnelling at curve section
				Pirastehfar et al. (2022)	GSS due to tunnel excavation that adjacent to existing tunnel
				Li et al. (2022)	GSS and deformation of existing tunnel induced by overlapped tunnelling
				Aswathy et al. (2022)	Tunnel geometry and soil elastic modulus on GSS in Young Alluvium Deposit
				Zhu et al. (2022)	GSS induced by tunnelling in saturated loess stratum
				Krishna and Maji (2022)	Comparison of empirical, analytical and numerical methods for predicting GSS
				Feng et al. (2022)	GSS caused by small-radius curved tunnel
				Hao et al. (2022)	GSS caused by twin-tunnel excavation under existing building
		Cam-Clay	Elastic	Zheng et al. (2022)	Soil-tunnel and tunnel-tunnel interactions of overlapping tunnels in soft ground
				Hou et al. (2022)	GSS caused by multi-line tunnelling with TBM in clay stratum
		HS and MC	Elastic	Vitali et al. (2022)	The influence of different construction schemes on GSS and face stability
				Ding et al. (2021)	GSS due to tunnelling in soil-rock composite strata
				Ma et al. (2022)	The influence of support pressure on GSS induced by TBM in soft-hard mixed strata
				Li et al. (2022)	Influence of excavation sequence on GSS
		HS	Elastic	Mu et al. (2021)	GSS and lining deformation in different soils
		CYsoil	Elastic	Do et al. (2022)	Influence of position and construction procedure of twin stacked tunnels on GSS
		CYsoil and MC	Elastic	Do et al. (2021)	The influences of TBM parameters on GSS
		Elastic-plastic-viscous model and MC	Elastic	Miao et al. (2021)	Analysis of time-dependent deformation behaviour of soil and GSS
	2D	MC	Elastic	Mohammadi and Azad (2021)	Purpose of making comparison with other GSS evaluation methods
		MC, soft soil model, soft soil creep model	Elastic	Zhu et al. (2022)	GSS caused by tunnelling in saturated loess stratum

MC means linear elastic with Mohr–Coulomb failure criterion, Cam-Clay includes original and modified Cam-Clay constitutive model, HS means hardening soil model, CYsoil is defined by a frictional Mohr-Coulomb shear envelope (zero cohesion) and an elliptic volumetric cap.

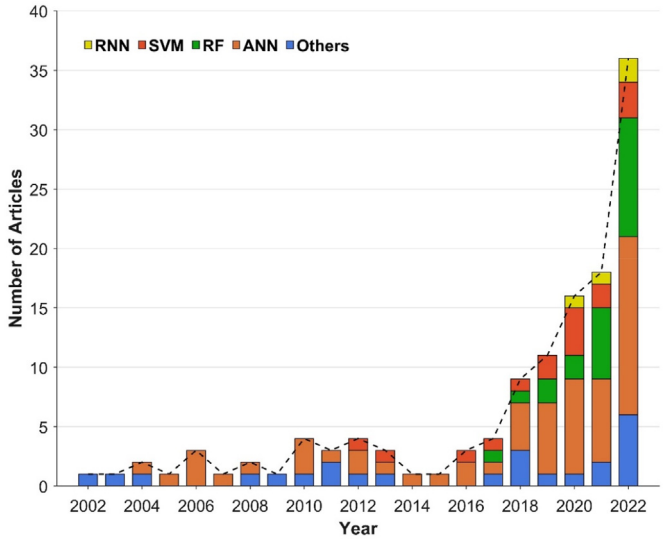

Fig. 4. The tendency of ML in ground movement and tunnel convergence problem.

engineering in the aspects of penetration rate forecast of tunnel boring machine (TBM), prediction of cutter life during tunnelling, analysis of tunnelling-induced GSS and convergence model of tunnel. Fig. 4 shows the trend of the application of ML in ground movement and tunnel deformation problem. As can be indicated, the number of published articles remains stable from 2002 to 2017 with a sharply increasing tendency in recent five years due to the development of AI technique. ANN is the most popular ML methods for GSS evaluation. ANN can automatically learn and extract useful features from raw data, and it learns by adjusting the weights of connections between neurons, which enables ANN to adapt to a wide variety of data structures. RF occupies the second dominant position. Unlike ANN and SVM, RF do not require input features to be scaled. It can handle mixed data types without the requirement of extensive preprocessing. GSS is also predicted by many other ML methods such as SVM, RNN, CNN, KNN etc. In fact, through data processing, all ML methods can identify the optimal target based on the given input. Their effectiveness depends on the nature of problems they are applied to and their accuracy levels.

3.1. Introduction to different machine learning methods

3.1.1. Artificial Neural Network (ANN)

ANN is a highly parameterized model that similar to the structure of animal brain. It is able to learn the pattern and find out the non-linear relationship between input and output variables by training and validation. An ANN consists of a set of simple information processing elements called neurons. As foundational units, these neurons help to carry the message from one cell to another cell. The arrangement of them determines the architecture of ANN (Mahdevari et al., 2012).

Fig. 5 illustrates the processing principle of ANN model. As can be seen, there are three layers in the ANN structure, including input layer, output layer and hidden layers. Every input has its individual weight. Each incoming signal (x_i) from previous layer is multiplied by an associated weight coefficient (w_{ij}). Then a summation function is applied and a bias (b_j) is added. This process is repeated for each layer until the final output is produced. Mathematically, the formula of output of each node is expressed as follows:

$$y_j = \sum_{i=1}^{n} w_{ij} \cdot x_i + b_j \tag{14}$$

Where y_j are outputs, w_{ij} are weights, x_i are inputs and b_j are bias.

For the hidden layers, it bridges inputs to outputs through non-linear transformation with linear combinations (Zhao et al., 2023). The simulation ability of ANN depends on the numbers of hidden layers mainly (Zhao et al., 2023). Each neuron output is regarded as input to next layer neurons. The commonly used activation function includes sigmoid, logistic, hyperbolic tangent (tanh) and rectified linear unit (ReLu) functions. The essence of ANN training is tuning weights through iterations until the error between the predicted values and real measurements is minimized. It means ANN can be iteratively trained many times to reduce the imperfection of the outputs (Armaghani et al., 2023). One challenge of ANN is that it has slow learning rate and may get trapped in local minima.

3.1.2. Decision trees (DT) and random forest (RF)

DT can be used for solving both regression and classification problems. The characteristic of DT is tree-like structure (Navada et al., 2011; Quinlan, 1990). As shown in Fig. 6, it contains root node, interior nodes as well as leaf nodes (Swain and Hauska, 1977). The root node and interior nodes are referred as nonterminal nodes, which are linked to decision stages; the leaf nodes represent final classifications (Navada et al., 2011; Podgorelec et al., 2002; Swain and Hauska, 1977). When a data point falls in a partitioned region, the decision tree classifies it as belonging to the most frequent class in that region (Kotsiantis, 2013). According to Kingsford and Salzberg (2008), DT is more interpretable than other classifiers such as SVM sometimes, because it combines straightforward questions in an understandable way. In addition, it can handle items with some missing features (Kingsford and Salzberg, 2008).

However, this algorithm is often suffered from the disadvantage of excessive complexity. And small variation of input data can lead to large changes in the construction of the tree (Kingsford and Salzberg, 2008; Kotsiantis, 2013). Some improvements have been proposed to optimize the performance of DT. For example, multiple DTs can be combined to reach a single output which is called Radom Forest (RF). RF can overcome the issue of overfitting effectively. It also increases the data volume that can be addressed. In classification problems, the output of RF is the

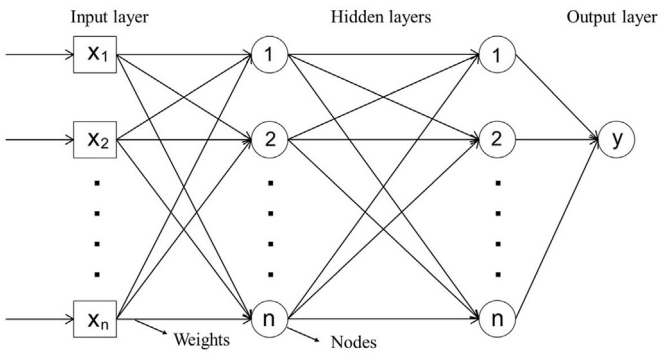

Fig. 5. The structure of Artificial Neural Network (ANN).

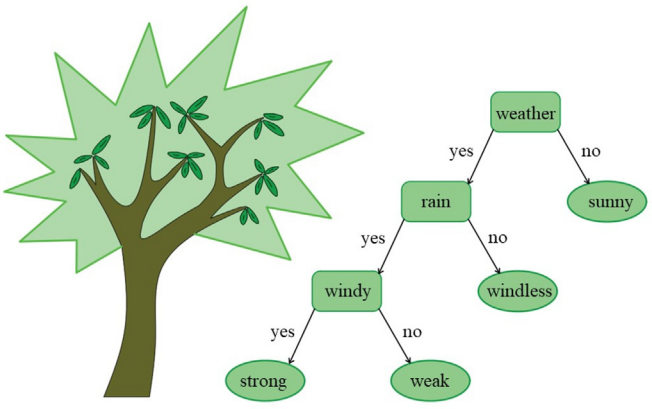

Fig. 6. The structure of Decision Tree (DT).

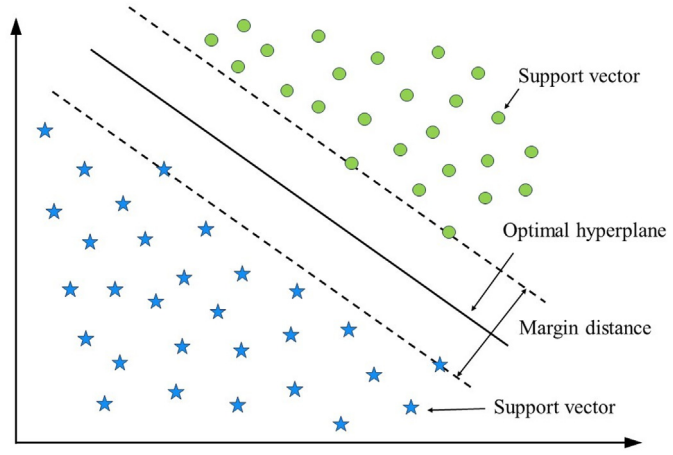

Fig. 7. An illustration of Support Vector Machine (SVM).

class selected by the majority of the DTs, while in regression tasks, the average predicted value of each DT is returned as the result of RF. Some other methods such as AdaBoost, XGBoost and Gradient Boost are suggested to cooperatively employed with RF. The principle of these boosting methods is combining a set of weak learners into a strong learner to minimize training errors and improve prediction accuracy. Although RF may lose the intrinsic interpretability of decision trees and might predict extreme values in continuous variables inaccurately, it presents better results in general.

3.1.3. *Support Vector Machine (SVM) and support vector regression (SVR)*

SVM is a supervised learning algorithm which can be used to deal with various classification and regression problems (Afradi et al., 2019; Meharie and Shaik, 2020). SVM seeks to maximize the margin between two classes, forming a hyperplane in the centre of the utmost margin (Akbarzadeh et al., 2022). The hyperplane is a decision boundary to classify the samples, and its location depends on the closest data points to the hyperplane (Zhao et al., 2023). This means the formed hyperplane ensures that the distance between it and the nearest data point of each class is maximized (see Fig. 7). The determination of hyperplane in 3D space can be accomplished by converting the data space with a set of mathematical functions known as kernels, including Gaussian, sigmoid, radical basis function and so on. To choose the appropriate kernel function and achieve a better performance of SVM, usually several trials have to be carried out (Zhao et al., 2023).

As SVM refers to both classification and regression methods, the term support vector regression (SVR) is applied for regression specially. SVR is an important branch of SVM. SVM tries to maximize the 'distance' to the nearest sample point of the hyperplane while SVR aims to minimize the 'distance' to the farthest sample point of the hyperplane. In addition, SVR adopts SVM to solve the problem of function approximation and regression estimation by introducing an alternative loss function (Mahdevari et al., 2012). In SVR, the main objective is finding the function that has the lowest deviation between the actual values and the predicted values, as shown in Fig. 8. As long as the deviation is less than ε, there is no penalty applied. However, the penalty function would be employed if the deviation is larger than ε.

SVM takes long training time for large data sets, therefore, it is not suitable for large datasets with many features. Furthermore, SVM is sensitive to the choice of parameters such as the regularization parameter and it is not easy to choose an appropriate kernel function.

3.1.4. *Recurrent Neural Network (RNN)*

RNN uses sequential data or time series data. It allows previous outputs to be used as inputs while having hidden states (Sherstinsky, 2020). As traditional neural networks cannot remember previous context, RNN is developed for handling temporal features especially. It is gradually occupying an important position in the field of image classification. As shown in Fig. 9, the characteristic of RNN is a loop structure. The message is delivered from one cell to the next in the hidden layer. RNN uses back propagation to update the weights of neurons. During forward propagation, the inputs move forward and pass through each layer to calculate output state. In back propagation, the message goes back and change the weights of neurons to make it learn better. Multiple RNN layers can be stacked to build deeper RNN, which can achieve better modelling capabilities. However, as the message is back propagated to lower layers, gradient often gets smaller, and eventually, the weights would remain unchanged at lower layers. This is the issue commonly suffered by RNN called gradient vanishing (Fei and Tan, 2018). RNN does not work effectively for learning long-term patterns and constructing deep network due to the gradient vanishing and exploding problems.

For each timestep, the activation $a^{<t>}$ and the output $y^{<t>}$ are expressed as follows:

$$a^{<t>} = g_1\left(W_{aa}a^{<t-1>} + W_{ax}x^{<t>} + b_a\right)$$

$$y^{<t>} = g_2\left(W_{ya}a^{<t>} + b_y\right) \tag{15}$$

Where $W_{aa}, W_{ax}, W_{ya}, b_a, b_a$ are coefficients that are shared temporally and g_1, g_2 are activation functions.

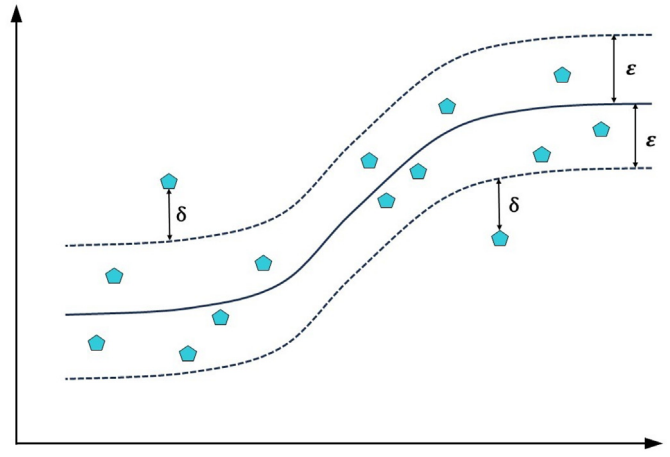

Fig. 8. An illustration of Support Vector Regression (SVR).

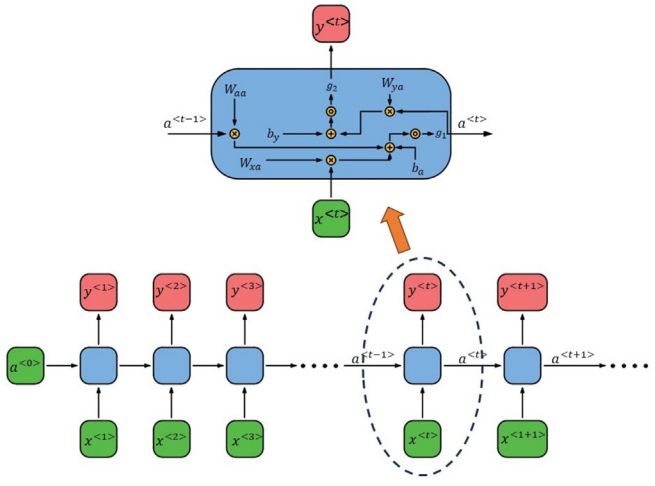

Fig. 9. The structure of Recurrent Neural Network (RNN).

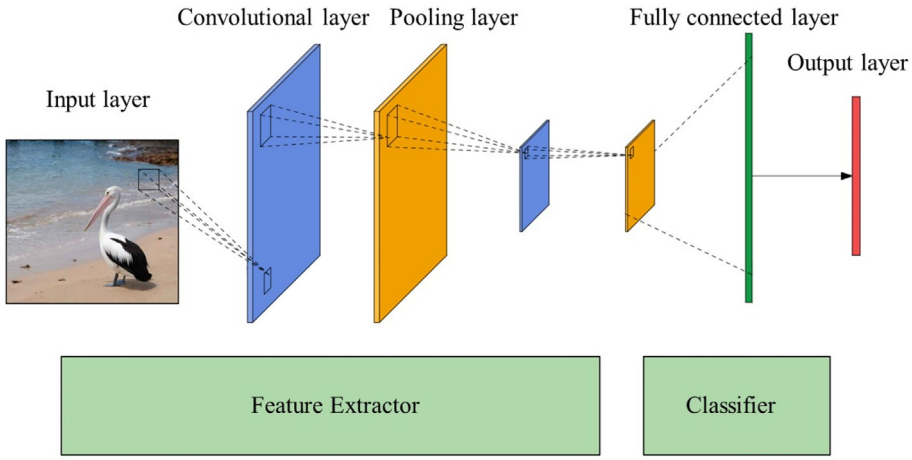

Fig. 10. The structure of Convolutional Neural Network (CNN).

3.1.5. *Convolutional Neural Network (CNN)*

CNN is a type of feed-forward artificial network. The main advantage of CNN is that it does not require human supervision for identifying important features and is relatively accurate at image recognition and classification. Typical CNN consists of several layers including input, convolutional, activation, pooling, dropout and output layers (see Fig. 10). These layers are mutually connected like neurons in a biological brain. The role of convolutional layer is recognizing features. An important element that constitutes the convolutional layer is the filter (Wang et al., 2021). Generally, there are more than one filter involved in a convolutional layer. Each convolutional filter of CNN slides across the input matrix with a definite stride (Chen et al., 2021). The convolutional filter and the stride size determine output size. The activation layer plays the role of increasing the nonlinearity of the convolution output. Chen et al. (2021) suggest implementing Rectified-Linear-Unit (ReLU) as activation function in CNN to get the reasonable gradient. For pooling layer, it can simplify the complexity of the network. This means pooling layer aims to compress the features of input, while reducing the number of parameters and dimensions of upper layers. A convolutional layer is often followed by a pooling layer, as convolutional layer produces multiple input matrices for the pooling layer (Wang et al., 2021). There are two pooling methods primarily: max pooling and average pooling. Their values are calculated by the maximum or mean operators, respectively. Both summarize the most activated and average presence of the input feature (Zhang et al., 2021). In terms of dropout layer, it can isolate the connections among different nodes randomly, as a result, achieves the goal of preventing overfitting problem.

Deep CNN models require a sizable volume of data to obtain good performance, which means the associated challenge of CNN is the lack of training data. In addition, due to the large number of parameters involved and complicated relationships in deep learning in CNN, the possibility of overfitting during the training phase is very high (Xu et al., 2019).

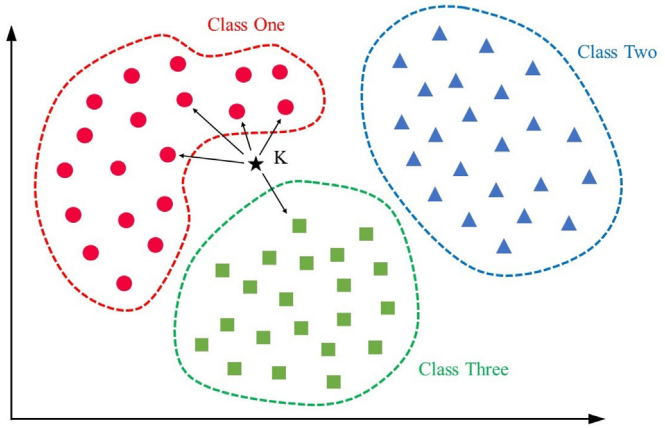

Fig. 11. The expression of K-Nearest Neighbors (KNN).

3.1.6. *K-nearest neighbors (KNN)*

KNN is a nonparametric, supervised learning classifier that uses proximity to classify or predict groups of individual data points. Based on the principle of local minimum of the target function, it aims to learn an unknown function of desired precision and accuracy. The core principle of KNN is predicting the label of a data point by the majority rule (see Fig. 11). It means the class of a data point is predicted by the dominant classes of its K most similar training data points (Zhang et al., 2017). KNN first selects K nearest training samples for a test sample, and then predicts the test sample with the major class among K nearest training samples (Deng et al., 2016).

There are two main issues of KNN required to be solved, which are the similarity measurement between two data points and the selection of K values, separately (Zhang et al., 2017). The value of K is regarded as an important and sensitive parameter for KNN. A small K value may lead to overfitting of KNN, while a large K may contribute to underfitting. In classification problem, KNN chooses the K value by setting a fixed constant for all data or performing cross-validation to estimate the value of K for each data point (Zhang et al., 2017). In regression problems, the output of KNN is the average values of the K nearest samples (Mahmoodzadeh et al., 2022).

3.2. *Performance evaluation metrics in machine learning*

ML methods are regarded as 'black-box' techniques since the internal prediction steps cannot be elucidated. Therefore, evaluation of machine learning performance is necessary. Performance analysis aims to display the validity and assess the accuracy of the established prediction models. Some reference parameters have been recommended to demonstrate the correspondence between predicted values and actual values. The evaluation metrics that have been commonly employed include the coefficient of determination (R^2), mean absolute error (MAE), mean absolute percentage error (MAPE), mean square error (MSE), root mean square error (RMSE) as well as variance account for (VAF). R^2 reflects the fitting level of the established model while MAE, MAPE, MSE, RMSE and VAF describe the differences between the predictions and measurements. In such case, MAE, MAPE, MSE, RMSE and VAF are also known as error parameters. Furthermore, in order to reveal the correlations between inputs and outputs clearly, Pearson correlation coefficient (R) is

proposed.

3.2.1. Pearson correlation coefficient (R)

The correlation between the measured and predicted data can be investigated by Pearson index (Chen et al., 2019; Zhang et al., 2020). It is a linear relationship fitting method. The expression of Pearson correlation coefficient (R) is shown in Equation (16). The number of R is in the range −1 to 1 that measures the strength and direction of the relationship between input and output variables.

$$R=\frac{n\sum_{i=1}^{n}x_iy_i-\sum_{i=1}^{n}x_i\sum_{i=1}^{n}y_i}{\sqrt{\sum_{i=1}^{n}x_i^2-\left(\sum_{i=1}^{n}x_i\right)^2}\sqrt{\sum_{i=1}^{n}y_i^2-\left(\sum_{i=1}^{n}y_i\right)^2}} \tag{16}$$

Where x_i is the value of input variable, y_i is the value of output variable, n means the total number of events considered.

3.2.2. Coefficient of determination (R^2)

Coefficient of Determination (R^2) is frequently employed to quantify the comparability between predicted and observed values. It represents the proportion of the variance in the dependent variable, which means it can reflect the overall fit of the established model. The formula of R^2 is expressed as Equation (17). Where y_i represents the ith measured value, y_i^* means the ith predicted value, and $\bar{y}$ is the mean value of the measured values. R^2 will increase with the improvement of model performance. This means if the predicted values accurately match the observed value, R^2 would close to 1.

$$R^2=1-\frac{\sum_{i=1}^{n}\left(y_i-y_i^*\right)^2}{\sum_{i=1}^{n}\left(y_i-\bar{y}\right)^2} \tag{17}$$

3.2.3. Variance account for (VAF)

Variance accounted for (VAF) is a measurement used in statistics and data analysis to evaluate how well a regression model can predict the outcome variables. Based on percentage, it is calculated as the proportion of variance in the dependent variable as shown in Equation (18). The perfect value for VAF is 100% for a model with $R^2 = 1$ and RMSE = 0.

$$VAF=\left[1-\frac{var\left(y_i-y_i^*\right)}{var\left(y_i\right)}\right]\times 100\% \tag{18}$$

3.2.4. Mean square error (MSE)

Mean square error (MSE) represents the deviation of the predicted results from the measured results. It is calculated by the average of the squares of the differences between the predicted and measured values. The definition of MSE is shown in Equation (19). As can be seen, this parameter is a non-negative value. With the improving of model performance, the value of MSE decreases.

$$MSE=\frac{1}{n}\sum_{i=1}^{n}\left(y_i-y_i^*\right)^2 \tag{19}$$

3.2.5. Root mean square error (RMSE)

Root mean square error (RMSE) declares the standard deviation of predicted results to the measured results (Equation (20)). It has the same tendency with MSE that with the improving performance of model RMSE value reduces. RMSE is better than MSE when the output values have different dimension, since RMSE maintains the same dimension as the output values.

$$RMSE=\sqrt{MSE}=\sqrt{\frac{1}{n}\sum_{i=1}^{n}\left(y_i-y_i^*\right)^2} \tag{20}$$

3.2.6. Mean absolute error (MAE)

Mean absolute error (MAE) reflects the mean magnitude of the errors. As can be indicated in Equations (20) and (21), RMSE and MAE have the same dimension. Since RMSE calculates errors by squaring, the obtained value of RMSE is larger than that of MAE generally. Additionally, different with RMSE, MAE is proportional to the absolute value of the error. Without considering the directions, each error influences MAE in proportion to its magnitude.

$$MAE=\frac{1}{n}\sum_{i=1}^{n}\left|y_i^*-y_i\right| \tag{21}$$

3.2.7. Mean absolute percentage error (MAPE)

Mean absolute percentage error (MAPE) is one of the widely used error evaluation metrics, which calculates errors between the predictions and the measurements and shows them in percentage expression (Equation (22)). As a dimensionless evaluation metrics, MAPE can compare the performance of different models on different datasets frankly. However, MAPE is not suitable for the situation when the measured values are very small even close to zero. The reason is MAPE would tend to infinity in that case.

$$MAPE=\frac{100\%}{n}\sum_{i=1}^{n}\left|\frac{y_i^*-y_i}{y_i}\right| \tag{22}$$

3.3. Machine learning performance optimization techniques

3.3.1. Data preprocessing

The quality of ML models is significantly impacted by the nature of input data. Applying preprocessing steps such as data standardization and normalization can scale the features of data to make them have similar scales. Data interpolation can fill in missing or incomplete information while data extraction can distil essential characteristics from complex datasets. Moreover, identifying and managing outliers contributes to the stability of ML models, and denoising techniques can help in reducing irrelevant fluctuations in datasets. Common feature selection methods include principal component analysis and correlation analysis mainly. Principal component analysis serves for dimensionality reduction. While identifying the principal components that have the greatest impact on the target variable, its primary objective is retaining the most critical information and minimizing the dimensions of data. Correlation analysis, on the other hand, focuses on identifying and eliminating highly correlated or redundant features in dataset. Removing these features can simplify ML model and improve its accuracy, as highly correlated features may lead to overfitting. It is notable that the effectiveness of preprocessing and feature selection techniques may vary across different ML models. For instance, tree-based models might be less sensitive to the scale of features, while SVM and ANN might require meticulous data normalization due to their sensitivity to the scaling and distribution of input data.

3.3.2. Generalization enhancement

Regularization and ensembling are two important techniques that can enhance the performance of ML models. Regularization prevents overfitting by adding a penalty term to the weight parameters of ML model, thereby improving its generalization. For example, dropout plays an important role in deep learning models, as it helps prevent overfitting by randomly dropping out a fraction of neurons during each training step. On the other hand, ensembling methods like RF can improve model performance by aggregating predictions from multiple weak learners, which reduces error rates on new data and enhances generalization capabilities. Furthermore, early stopping is a universal strategy used to minimize overfitting across all types of ML models. It continuously monitors the performance of the model on the validation set during the training process. Once it is detected that this performance is starting to

drop, training will be terminated early to avoid the model from overfitting. Cross-validation and bootstrapping are two techniques used to assess the generalization ability of ML models. Cross-validation partitions the original dataset into multiple subsets, using one as the validation set and the remainder for training. This cycle is repeated with different subsets to provide a more generalized and robust evaluation. In contrast, bootstrapping involves random sampling with replacement from the original dataset to generate multiple resampled sets for training and evaluation. These two methods identify potential issues of overfitting or underfitting, improving the reliability of ML models.

3.4. The application of different machine learning methods in predicting ground settlement

VOSviewer program was employed for generating keyword distribution and the relationship among them. Fig. 12 shows the distribution of keywords in the application of ML for predicting GSS. The size of each circle corresponds to the frequency of keyword occurrences, which means a larger circle represents a higher frequency. The thickness of the lines signifies the strength of the relationship between keywords. A thicker line denotes a more significant relationship, while a thinner line indicates a weaker association between two points. As can be seen, the keyword with the highest occurrence frequency is ‘ground settlement’, which is primarily represented by terms such as surface settlement, ground movements, ground deformations and subsidence. The keywords with the second highest frequency are 'tunnels' and ‘forecasting’, which are associated with terms like tunnelling, shield tunnelling, tunnel excavation, TBM, prediction and so on. Compared with rock and other ground condition, shallow tunnelling in soft clay environment has gained significant attention. Interrelationships among ground settlement, tunnels, soils, foresting and machine learning are stronger than other keywords. Limited connection linked between some keywords such as railway construction, retaining wall and soft rock.

As different researchers employ different factors for analysing GSS problem, the number of parameters is huge and diverse. Such a large number of inputs with various considerations makes it challengeable to grasp the important information. Those inputs can be briefly grouped. For example, five catalogues of influence factors are suggested as follows for the prediction of GSS: tunnel geometry, geotechnical parameters, TBM operations parameters, hydraulic factor and others. Detailed information can be found in Appendix A. Also, some convertible parameters have been restructured to match a general expression. For example, unit weight and density of soil can be used interchangeably, which is expressed by soil density uniformly. Tunnel depth below water table and water level can be summarized by water table. Cover-span ratio is simply represented by cover and tunnel diameter, separately. Advance rate and penetration rate of a TBM share the same unit, both signifying the speed at which the machine moves forward. They are represented with excavation speed (ES) in this paper.

Since tunnel may pass through stratum with different soil layers, ‘soil types’ represents the variation of ground materials such as soil type and rock composition around tunnel (crown, invert, face). While most soil parameters are sourced from laboratory test and in-situ measurements, only a limited number of authors utilize average values of all soil layers as

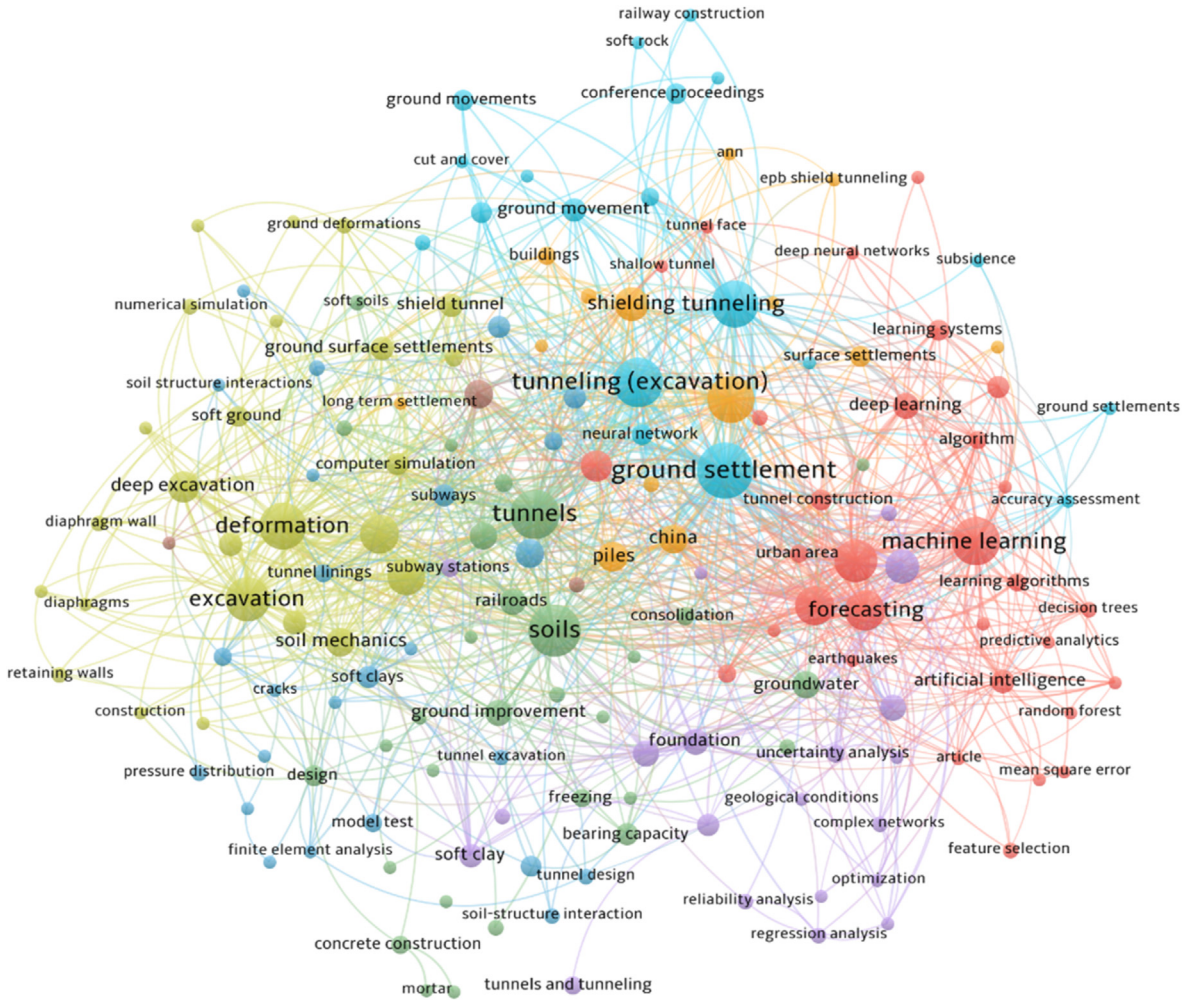

Fig. 12. Keywords network of tunnelling-induced GSS by ML methods.

the inputs. When the dataset is relatively small and insufficient, average values for soil parameters are typically adopted as a workaround.

Fig. 13 displays the frequency of variables employed for GSS prediction (such as service as input in ML). A larger word indicates a higher frequency of use. For soil features, friction angle and cohesion are considered as the most important factors influencing tunnel and ground deformation (see Fig. 13). Both can be evaluated from laboratory tests or in-situ SPT tests. These two parameters characterize the strength and stability of soil and soil resistance to disturbance. Soil density, Young's modulus and Poisson's ratio are obtained from laboratory tests primarily. Uniaxial compressive strength tests (UCS), dynamic penetration tests (DPT) and standard penetration tests (SPT) are commonly employed to obtain soil and rock properties in site. Among them, SPT is used most frequently. The data from these three tests can be applied for ML, eliminating the need for additional laboratory tests.

As can be summarized in Fig. 13, the most used TBM operation parameter is excavation speed, followed by face pressure, thrust and torque. Grouting pressure and grouting filling volume are also regarded as important factors influencing GSS as they determine the filling status of the gap between tail and liner. Operation of TBM induces soil volume loss inevitably, which subsequently triggering deformation of tunnel profile and consequential ground displacement. Excavation speed and face pressure have been regarded as two critical factors associated with GSS. During tunnelling process, if excavation speed of TBM is high while the chamber pressure is low, the rate at which soil is expelled would exceed the rate of replenishment, leading to an imbalance. As a result, GSS may occur. On the other hand, if the excavation speed is slow but the face pressure remains high, it can trigger ground heaving due to the excess pressure exerted on the surrounding soil. Other researchers also incorporate additional parameters in their unique studies such as deviation, pitching angle and stoppage of TBM. While those unique parameters can have a certain degree of influence in specific projects, their overall contribution tends to be less significant when compared to the commonly recognized factors.

In terms of tunnel geometry, tunnel depth is a critical factor, especially in research studies focusing on tunnels with a consistent diameter. While some researchers utilize cover depth instead of tunnel depth, these two parameters are interchangeable. In addition, common considerations often include the water table and the thickness of soil layers. Sometimes considerations can extend to distance form tunnel face and settlement markers and rock layer thickness. For other associated factors, the time factor due to creep and consolidation of soil is the most frequently factor. Surface load and construction method are sometimes taken into account.

Fig. 14 shows the distribution of ML applications in predicting GSS within past ten years. It illustrates that ANN is the most popular approach for GSS analysis, followed by RF and SVM. RNN takes the fourth place. Adaptive Neuro-Fuzzy Inference System (ANFIS), Multivariate Regression (MR), Gaussian Processes (GP), KNN, CNN and other ML methods collectively account for only 14% of the methods applied. This discrepancy can be attributed to the considerations of both accuracy and computational efficiency. The algorithms and internal structures of ANN and RF are more complex than simple ML methods such as KNN. Owing to their strong performance and well-established reliability in managing intricate and diverse data, ANN and RF are frequently chosen for predicting GSS. While SVM was a research point for GSS estimation a few years ago, deep learning models such as CNN have demonstrated their effectiveness and emerged as powerful tools for evaluating GSS recently. Compared with other methods, the application scope of KNN is restricted. Only two of 103 statistical articles apply KNN. For more details regarding the application of ML in GSS prediction, the statistical main outcomes from the past decade can be found in Appendix A.

4. Discussion

4.1. Ground surface settlement in different tunnel construction stages

The process of GSS is long lasting, which may take decades to reach a stabilisation (Shen et al., 2014). It happens from the beginning of tunnel

Fig. 13. Influencing factors of GSS caused by tunnelling. (a) geotechnical parameters (b) TBM operation parameters (c) tunnel geometry and (d) other factors.

excavation and keeps developing after tunnel construction is completed. Analysis of GSS is challenging as there are a lot of factors that impact GSS. Generally, the influencing factors can be categorized into tunnel geometry, geotechnical parameters, and TBM excavation operations. For long-term settlement prediction, ground properties and tunnel geometry are predominantly influential, whereas construction methods tend to be the key determinants for short-term GSS analysis.

During tunnelling process, the natural stress state of ground is disturbed, leading to potential surface subsidence. Initially, a relatively stable stress equilibrium exists within the ground, maintained primarily by soil weight and groundwater. The weight of soil induces vertical stress, increasing progressively with depth. Groundwater creates pore water pressure, affecting soil stability and altering its physical and chemical properties. Tunnel excavation disrupts this original state of stress balance, causing stress redistribution and various ground issues such as deformation, cracking and changes in groundwater level. These changes can consequently lead to GSS. For example, the fluctuation of groundwater level contributes to consolidation and creep of soil, further exacerbating GSS issues (Shen et al., 2014). Tunnel construction method also has significant impacts on GSS. For instance, when using a TBM, the tail void (space between cutter head and lining segment) needs to be carefully managed. Grouting is an effective technique to fill the tail void and mitigate GSS. For optimal results, grouting pressure needs to be controlled and calibrated to ensure sufficient filling and compaction, avoiding causing excessive stress on the surrounding soil. Also, the grouting material should possess sufficient flowability to adequately fill the void. Other properties of grouting material such as viscosity, strength and consolidation time should be tailored to suit individual ground conditions. Face pressure of TBM is another important factor influencing transverse and longitudinal GSS. As mentioned before, the excavation speed (advance rate or penetration rate) should keep balance with cuttings transport speed to avoid heaving or subsidence of ground surface in longitude direction.

The completion of a tunnel construction project does not signify the end of GSS. Post-construction factors can continue to influence GSS, with the gravitational force of liner and changes in underground water level being prime contributors. The gravity of liner can result in soil consolidation, potentially contributing to GSS. Magnitude of this effect is influenced by the weight and material of the liner, as well as the depth and size of tunnel. Heavy rain, drainage and potential leakage of liner present risk on GSS in many aspects (Shen et al., 2014). For example, intense or prolonged periods of rainfall can lead to an increase in groundwater levels, which can exert additional pressure on soil and tunnel structure. The saturation of soil due to heavy rain can also reduce its shear strength, making it more susceptible to deformation and settlement. Wu et al. (2015) proposed that the shear stiffness between rings can also contribute to GSS from long-term of view. Thus, it is important to maintain supervision and monitoring of GSS after tunnel construction is completed.

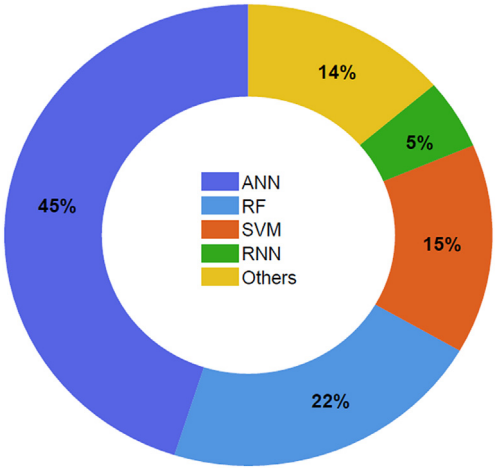

Fig. 14. Percentage of different ML methods in GSS problem within past ten years.

4.2. *Discussion of different tunnelling-induced ground displacement evaluation methods*

According to Web of Science and Scopus, a total number of 677 articles that published between 2013 and 2022 were reviewed. The keywords for literature searching include 'tunnel', 'tunnelling', 'ground surface', 'ground movement', 'deformation', 'displacement', 'settlement', 'empirical', 'analytical', 'numerical', 'FEM', 'FDM', 'artificial intelligence', 'machine learning', 'neutral network', 'soft computing', 'deep learning', 'AI', and 'ML'. There were 103 articles explored the application of ML in tunnel stability, tunnel deformation and ground movement problem. In the same period, 51 articles utilised empirical methods, 86 delved into analytical methods, and a notable 437 articles employed numerical approach statistically.

As shown in Fig. 15, numerical method holds the predominant share (65%) among the four methods utilised for ground and tunnel deformation analysis. Some computer simulation software such as ABAQUS, PLAXIS and FLAC3D has been developed to simplify the process of material property definition, model simulation and computational activities. These software packages enable fairly estimation of GSS prediction. The key constraint faced by numerical method is computational cost (see Table 4). The computational demands can be substantial, particularly for complex geological conditions. This limitation can sometimes make numerical methods less feasible for real-time and rapid assessments. Empirical method occupies the smallest percentage which is 8%. The empirical formulas are developed in early stage based on engineering experience and site observation, which means the application range and considered parameters are limited. In addition, AI method takes the second place, followed by analytical method (see Fig. 15). Since analytical method is relatively more accurate and has wider scope of application than empirical method, it is adopted as an effective method to deal with GSS problem. As a developing approach, AI offers a new direction for analysing GSS problem accurately. By leveraging complex algorithms and data-driven learning, AI techniques are becoming increasingly adept at evaluating the intricate variables that contribute to GSS.

Compared with long-time supervision of GSS in site, laboratory experiment is time-efficiency. The interaction between tunnel and nearby structures can be modelled easily (Loganathan et al., 2000). And different materials and construction methods can be tested and compared in laboratory. However, laboratory test cannot reflect the in-situ behaviour of ground and tunnel due to size effect. On the one hand, the mechanical properties of soil or rock in the laboratory may not exactly match those in the field. The grain size of soil relative to tunnel diameter is a significant factor. In a small-scale model, the relative size of the soil particles may be larger compared to the tunnel diameter, affecting the interaction between soil and tunnel (Idinger et al., 2011). On the other hand, the test apparatus introduces boundary effects that can significantly influence the results of laboratory experiment. For example, the container walls restrict lateral movement of soil, potentially leading to stress concentration near the boundaries. The confinement of the sample within the apparatus walls can restrict the natural deformation behaviour of the soil, while introducing friction. This friction can influence the shearing behaviour of soil. In tunnelling scenarios, boundary condition effects can turn into inaccurate descriptions of how the ground settles. The size and shape of the test apparatus play an important role in how significantly boundary effects influence test results. Smaller containers may exhibit more pronounced boundary effects. Normally, laboratory experiment is validated by numerical simulation or established formulas.

ML gains popularity in recent years in geotechnics due to its powerful capabilities and versatile adaptability. Some improved algorithms are

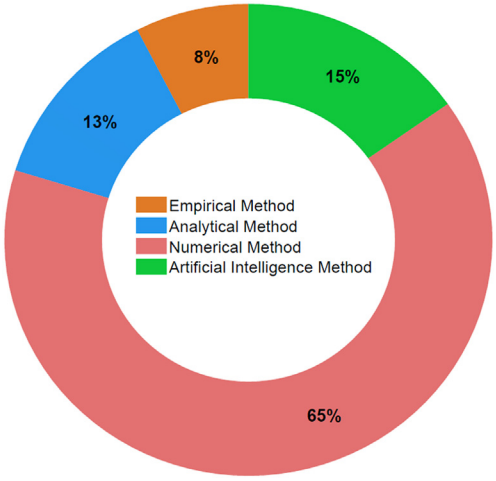

Fig. 15. The percentage of different methods on tunnel and ground deformation analysis from 2013 to 2022.

proposed to optimize the selection of hyperparameters of traditional algorithm, such as particle swarm optimization (PSO), imperialist competitive algorithm (ICA) and whale optimization algorithm (WOA). Those studies achieve an outstanding GSS prediction in special tunnel projects. PSO is inspired by the intricate social behaviors observed in bird flocking or fish schooling (Hajihassani et al., 2018; Li et al., 2014). Within PSO, a swarm of particles navigates through the search space, collaboratively working to pinpoint the optimal solution. ICA draws its inspiration from the concept of imperialistic competition, wherein nations are categorized into colonies and imperialists, with the imperialists vying to assert dominance and acquire colonies (Hosseini and Al Khaled, 2014). WOA is based on the bubble-net hunting strategy employed by humpback whales (Deng et al., 2023). In this algorithm, agents mimic the sophisticated hunting patterns and strategies of whales to optimize the search process. Their advantages and limitations are briefly summarized in Table 5.

4.3. *Challenges of machine learning in ground surface settlement prediction*

ML faces some challenges in the realm of tunnel-induced GSS prediction (see Table 4). A primary issue is generalization. ML model might excel in forecasting ground surface shifts for a tunnel project under specific geological conditions, its adaptability to diverse situations is often limited. This restricted scope implies that each ML model can usually only analyse a particular tunnel project, but no model has yet demonstrated universal applicability. In other words, although a ML model may perform well on a specific task, its ability to generalise to different tasks still needs to be improved. Another hurdle is the opacity of ML algorithms. Deep learning models, for example, are exceptionally powerful but suffer from a "black box" problem that makes them difficult to interpret. This becomes problematic when understanding that different datasets and their structures can have significant impacts on model prediction. The measured datasets for GSS are often insufficient due to the spatial-temporal variability of GSS problem. On the one hand, since ground properties change above tunnel as well as at tunnel face, GSS varies both longitudinally and transversely along tunnel. On the other hand, each point above tunnel may experience different movement with time, which means subsidence of ground surface does not vary uniformly over time. As a result, the actual ground movement datasets are difficult to be gathered. The quality and availability of input data also constrains ML model performance, especially when noise, missing values, and bias are prevalent, which introduces another layer of complexity (Suwansawat and Einstein, 2006).

In addition, the range of considered input variables varies widely across studies, contributing to a complicated and fragmented research landscape. For instance, some researchers such as Ahangari et al. (2015), Zhou et al. (2016) as well as Ghiasi and Koushki (2020) emphasise the significance of tunnel depth and diameter, integrating these parameters with selected soil properties to analyse GSS. By not accounting for tunnel construction method and employing an incomplete set of soil parameters, these studies inadvertently limit the comprehensiveness of their analysis. Some other researchers argued for the importance of other factors like groundwater levels and tunnel construction methods. The performances of TBM and grouting operations are regarded as essential factors for ground movement. For example, penetration rate, advance rate, excavation speed, torque, thrust, chamber pressure, grouting filling volume and grouting pressure are commonly included under consideration. However, some of them take limited consideration of soil characteristics such as Wang et al. (2013), Bouayad and Emeriault (2017), Goh et al. (2018), Kannangara et al. (2022), Cheng et al. (2022, 2023), while some others take simplified parameters to represent soil properties such as

Table 4
Advantages and limitations of methods for predicting tunnelling-induced ground settlements.

Category	Advantages	Limitations
Empirical Method	1. Easy to understand and implement 2. Provide quick approximations 3. Useful to make comparison with other methods 4. Provide initial idea for estimating GSS	1. Few factors are considered 2. Results are not highly accurate 3. Limited applicability to different and complex underground conditions 4. Ignore the influence of different tunnel construction techniques and 3D effects 5. Cannot predict horizontal displacement
Analytical Method	1. Relatively simple formulas 2. Cover both horizontal and vertical displacements 3. Relationship between affecting parameters could be understood.	1. Employing simplified assumptions 2. Only applicable for specific types of ground conditions 3. Time-dependent consolidation and creep of ground are ignored
Numerical Method	1. Achieve graphic visualization 2. Can simulate tunnelling process 3. Highly adaptation to various ground conditions and solve complex problems 4. Take more parameters and soil-tunnel interaction into consideration	1. Time-costing 2. Sensitive to boundary condition 3. Hard to verify and validate results 4. Accuracy highly depends on constitutive model of soil
AI Method	1. No need prior knowledge 2. High accuracy 3. Capable of capturing multiple factors and complex interactions among them 4. Can process various types and structures of data, including geological information, TBM parameters, etc.	1. Quality relies on data heavily 2. High computational cost 3. Complicated algorithm and poor interpretability 4. Poor generalization to different ground conditions and construction techniques

Table 5
The advantages and disadvantages of PSO, ICA and WOA optimization algorithm.

Algorithm	Advantages	Limitations
PSO	1. Fast convergent 2. Simple algorithm and easy to understand 3. Promising performance on nonlinear function optimization	1. Easy to fall into local optimum 2. Premature and divergence issue
ICA	1. Good convergence rate 2. Flexibility, robustness and scalability 3. Powerful in handling large number of decision variables	1. Premature convergence issue 2. Many parameters tuning required 3. Lacks theoretical convergent properties
WOA	1. Low computational cost 2. Small number of predetermined parameters 3. Can avoid local optima and get a globally optimal solution	1. Slow convergence speed 2. Falls into local optimal value easily 3. Low precision

Zhang (2019), Chen et al. (2019), Zhang et al. (2020), Tang and Na (2021), Feng and Zhang (2022) and Liu et al. (2022). They concentrated on GSS caused by TBM performance but neglected the influence of soil properties on GSS in a certain degree. Given the diversity of perspectives, it is evident that there is no consensus on which factors are most pivotal for inclusion in GSS analysis models. A holistic model that can adequately represent the multifaceted influences on GSS is lacking.

4.4. Recommendations and future work

Take several parameters to represent ground condition is not adequate. The author suggests employing more soil parameters in conjunction with in-situ tests to indicate soil behaviours accurately. Laboratory tests of soil properties should involve Young's modulus, Poisson's ratio, cohesion, friction angle, unit weight etc. Meanwhile, in-situ assessments should encompass SPT, DPT and UCS, as they reflect different features of geotechnical materials. In some cases, like highly expansive clay, the permeability, expansion coefficient and moisture content should be considered as well. For tunnel geometry, the tunnel depth, tunnel diameter and groundwater level are three important factors that need to be considered. For cases where nearby buildings exist, more parameters such as the distance from the building to tunnel centreline should be included. There are many parameters regarding TBM performance that can be taken into consideration, including torque, thrust, penetration rate, face pressure, grouting filling volume and grouting pressure. Other parameters like advance rate, rotation speed and specific energy can be calculated and converted through the front primary parameters. Furthermore, some occasional dynamic factors such as the temporarily increasing of ground water level due to heavy raining, additional loading on the ground and repeated vibration should also be included in some situations. Although some other parameters such as temperature change may affect soil behaviour and influence tunnel convergence further, these can be omitted due to their small contributions.

Considering the difficulties and costs associated with gathering field data for GSS, computer simulations can provide a complementary source of high-quality, controlled data to train and validate ML models. This synergy could result in more robust and accurate models, as simulations can replicate a wide range of tunnelling and geological conditions that are challenging to capture in field data alone. The ML algorithms could also be designed to become more adaptive, learning in real-time from new data as a tunnelling project progress. This would enable dynamic updating of predictions, thereby offering more timely and accurate guidance for construction and mitigation efforts. Additionally, the development of transparent interpretable ML models is necessary, which could aid in identifying the most influential factors in GSS, thereby guiding both the engineering practices and policy decisions. Another avenue for research is to focus on optimising the trade-offs between model complexity and computational efficiency. Having an ML model that can deliver quick yet accurate predictions could be highly beneficial. Advanced ML models such as CNN, RNN and transform algorithm, can be computationally intensive, thereby consuming considerable time and resources. This creates a dilemma where a more accurate model might be less feasible to employ in real-world scenarios due to its computational demands. Researchers could explore various approaches to address this challenge, such as model pruning, quantization, or the adoption of more efficient algorithms that provide a good balance between accuracy and computational speed. Techniques like transfer learning could also be considered, where a pre-trained model is fine-tuned for the specific task of GSS prediction, thereby reducing the computational burden. More recommendations can be found in Table 6. Future work should aim to create a blend of ML and computer simulation, develop adaptive and interpretable ML algorithms, explore multimodal learning, and fine-tune the balance between computational complexity and efficiency.

Table 6
Suggestions for laboratory tests, numerical and artificial intelligence methods.

Category	Recommendations
Laboratory Experiment	1. Appropriate scale modelling 2. Careful selection of experimental geotechnical materials 3. Calibration of measurement tool 4. Consider multiple factors to model actual field conditions 5. Validation of results
Numerical Method	1. Establish detailed geological condition 2. Appropriate selection of soil and rock constitutive models 3. Account for sensitivity analysis (influence of different parameters) 4. Validation of results
AI Method	1. Qualified input data 2. Use optimization and generalization techniques 3. Employ more advanced algorithms 4. Combined with numerical methods

5. Conclusion

The prediction of GSS faces challenges due to its internal complexity and the multitude of influencing factors. In this study, the assumptions, principles, application conditions, strengths and limitations of multiple GSS evaluation methods are summarized, with a focus on AI approach. Traditional GSS evaluation methods consider part of the influencing factors and provide a fundamental estimation of GSS. They are criticized for accuracy or validation concerns. As a powerful tool for identifying optimal solutions, AI has gained widely usage in geotechnical engineering. ML can learn from historical data, effectively addressing the limitations of traditional methods by involving a broader range of factors. Despite of its advantages, the application of ML requires caution in terms of generalization and accuracy, as it can lead to underfitting or overfitting issues. In addition, the quality of ML model relies on input data significantly. Therefore, data preprocessing and feature selection play pivotal roles in developing robust ML models for GSS prediction. By cooperating with numerical simulation, advanced ML models can overcome the restriction of data shortages. The establishment of open-assessed data repository are recommended to be applied for the training of advanced ML models to enhance the accuracy and reliability of GSS prediction.

CRediT authorship contribution statement

Gang Niu: Investigation, Methodology, Software, Writing – original draft. **Xuzhen He:** Supervision, Validation, Writing – review & editing.

Haoding Xu: Software, Validation, Writing – review & editing. **Shaoheng Dai:** Validation.

Declaration of competing interest

The authors declare that they have no known competing financial interests or personal relationships that could have appeared to influence the work reported in this paper.

Appendix

Ground Condition	Input														
	Geometry				Geotechnical Properties										TBM Operation Parameters
	Tunnel Depth (H)	Cover Depth (C)	Tunnel Diameter (D)	Others	Young's Modulus (E)	Compression Modulus (Eo)	Cohesion (c)	Friction Angle (φ)	Soil Density (ρ)	Standard Penetration Test	Dynamic Penetration Test	Unixal Compressive Strength Test	Moisture Content (ω)	Other Geotechnical Parameters	Excavation Speed
Soil	–	✓	–	–	✓	–	–	–	–	✓	–	–	✓	–	✓
	✓	–	✓	Distance between tunnels etc.	–	–	–	–	✓	✓	u	–	–	Soil types	✓
	✓	–	–	Distance from tunnel face to monitor	–	–	–	–	–	–	–	–	–	Soil types	✓
	✓	–	–	–	✓	–	✓	✓	✓	–	–	–	–	Soil types	–
	✓	–	✓	–	✓	–	✓	✓	–	–	–	–	–	–	–
	✓	✓	✓	Distance from tunnel face to monitor	–	–	–	–	–	–	–	–	–	Soil types	✓
	✓	–	✓	Volume loss etc.	–	–	✓	–	–	–	–	–	–	–	–
	✓	–	✓	–	–	✓	✓	✓	–	–	–	–	–	–	✓
	–	✓	–	–	✓	–	–	–	–	✓	–	–	✓	–	✓
	✓	–	✓	–	✓	–	✓	✓	–	–	–	–	–	–	✓
	–	–	–	–	✓	–	✓	–	–	–	–	–	–	Earth pressure coefficient	–
	✓	✓	✓	Soil layer thickness at crown, invert etc.	–	–	–	–	–	–	–	–	–	Soil types	–
	✓	–	–	–	✓	–	✓	✓	✓	✓	–	–	–	Poisson's Ratio	✓
	✓	–	✓	–	✓	–	✓	✓	–	–	–	–	–	–	–
	–	✓	–	–	✓	–	–	–	–	✓	–	–	✓	–	✓
	–	✓	✓	Distance of building to tunnel etc.	–	✓	✓	✓	–	–	–	–	–	–	✓
	–	✓	–	–	–	–	✓	✓	–	–	–	–	–	–	✓
	✓	–	✓	Volume loss etc.	–	–	✓	–	–	–	–	–	–	–	–
	–	✓	✓	Tunnel inclination	–	–	✓	✓	✓	–	–	–	–	–	–
	✓	–	–	Distance from tunnel face to monitor	–	✓	–	–	–	–	–	–	–	–	✓
	–	✓	–	–	–	–	–	–	–	–	–	–	–	Soil types	✓
	✓	–	–	–	–	✓	✓	✓	✓	–	–	–	–	–	✓
Soil and				Mixture	–	✓	–	–	–	–	–	–	–	✓	✓
Rock	200	ANN	–	Chen et al. (2019)											
	–	✓	–	–	–	–	–	–	–	✓	✓	✓	–	–	✓
	–	✓	–	–	–	–	–	–	–	✓	✓	✓	–	Soil types	✓
	–	✓	–	–	–	–	–	–	–	✓	✓	✓	–	Soil types	✓
	–	–	–	Thickness of soil and rock layers etc.	–	–	–	–	–	–	–	–	–	–	✓
	–	✓	–	–	–	–	–	–	–	✓	✓	✓	–	Soil types	✓
	–	✓	–	–	–	–	–	–	–	✓	✓	✓	–	Soil types	✓
	–	✓	–	–	–	–	–	–	–	✓	✓	✓	–	Soil types	✓
	–	✓	–	–	–	–	–	–	–	✓	✓	✓	–	Soil types	✓
	–	✓	–	–	–	–	–	–	–	✓	✓	✓	–	Soil types	✓
	–	✓	–	–	–	–	–	–	–	✓	✓	✓	–	Soil types	✓
	✓	–	–	Soil layer thickness at crown, invert etc.	–	–	–	–	–	✓	–	–	–	Soil types	–
	–	✓	–	Thickness of soil and rock layers etc.	–	–	–	–	–	–	–	–	–	–	✓
–	✓	–	–	–	–	–	✓	–	–	–	✓	–	–	✓	✓

ANN is artificial neutral network, RF is random forest, SVM is support vector machines, RNN is recurrent neural network, KNN is K-nearest neighbors, MR is multivariate regression, ANFIS is adaptive neuro-fuzzy inference, GP is Gaussian processes. BA means boruta algorithm, GA means genetic algorithm, PSO means particle swarm optimization, ICA means imperialist competitive algorithm, WOA means whale optimization algorithm, GEP means gene expression programming.

Input											Datasets	ML methods	Optimization Algorithm	References
TBM Operation Parameters									Hydraulic	Others				
Face Pressure	Thrust	Torque	Grouting Filling	Grouting Pressure	Rotation Speed	Pitching Angle	Stoppage	Others	Water Table					
✓	–	–	–	✓	–	–	–	–	–	–	148	ANN, MR	–	Zhang and Goh (2013)
✓	–	–	✓	–	–	–	–	Earth volume	✓	–	230	ANN, SVM, GP	–	Ocak and Seker (2013)
✓	–	–	✓	✓	–	✓	–	–	✓	–	661	ANN, SVM	–	Wang et al. (2013)
–	–	–	–	–	–	–	–	–	–	–	17	MR	–	Mohammadi et al. (2015)
–	–	–	–	–	–	–	–	–	–	–	53	ANFIS, MR	GEP	Ahangari et al. (2015)
✓	–	–	✓	✓	–	✓	–	–	✓	–	661	ANN, SVM	–	Wang et al. (2016)
–	–	–	–	–	–	–	–	–	✓	Construction methods	40	RF	–	Zhou et al. (2016)
–	✓	–	✓	✓	–	–	–	–	–	–	26	RF	–	Zhou et al. (2016)
✓	–	–	–	✓	–	–	–	–	–	–	148	ANN, MR	–	Goh et al. (2018)
–	✓	–	✓	✓	–	–	–	–	–	–	41	ANN, ANFIS	–	Moeinossadat et al. (2018)
–	–	–	–	–	–	–	–	–	–	–	143	ANN, MR	ICA	Moghaddasi and Noorian-Bidgoli (2018)
–	–	–	–	–	–	–	–	–	–	–	500	SVM	–	Zhang et al. (2019)
–	–	–	–	–	–	–	–	–	–	–	123	ANN	PSO	Hajihassani et al. (2020)
–	–	–	–	–	–	–	–	–	–	Construction methods	300	ANN, RF, SVM, KNN	–	Mahmoodzadeh et al. (2020)
✓	–	–	–	✓	–	–	–	–	–	–	148	ANN, RF, SVM, MR	–	Zhang et al. (2021)
✓	✓	✓	✓	–	✓	–	–	–	–	Foundation intergrity and building intact status	500	ANN	–	Pan and Zhang (2022)
✓	✓	✓	✓	✓	–	–	–	Earth volume	–	–	533	ANN, RF, SVM	–	Su et al. (2022)
–	–	–	–	–	–	–	–	–	–	Construction methods	38	ANN	PSO	Kong et al. (2022)
✓	–	–	–	–	–	–	–	–	✓	Surface surcharge	250	SVM	PSO	Mahmoodzadeh et al. (2022)
–	✓	✓	–	✓	✓	–	–	Discharge flow rate etc.	✓	–	187	ANN, RF, SVM, MR	–	Liu et al. (2022)
✓	✓	✓	–	–		–	–	Jack pressure etc.	✓	–	264	RF	BA	Kannangara et al. (2022)
✓	✓	✓	✓	✓	✓	–	–	–	–	–	370404	ANN, RNN	WOA	Ge et al. (2022)
✓	✓	✓	✓	–	–	–	–	–	✓	–	200	ANN	–	Chen et al. (2019)
✓	✓	✓	✓	–	–	–	–	–	✓	–	200	ANN, RF, SVM	–	Chen et al. (2019)
✓	✓	✓	✓	–	–	–	–	–	✓	–	294	RF	–	Zhang (2019)
✓	✓	✓	✓	–	–	–	✓	–	✓	–	294	RF	PSO	Zhang et al. (2019)
✓	✓	✓	✓	✓	–	–	–	Tail void etc.	✓	Karst cave treatment scheme	328	ANN	ADAM	Zhang et al. (2020)
✓	✓	✓	✓	–	–	–	✓	–	✓	–	294	ANN, RF, SVM	PSO	Zhang et al. (2020)
✓	✓	✓	–	–	✓	–	✓	–	✓	–	396	RF, RNN	–	Zhang et al. (2020)
✓	✓	✓	✓	–	–	–	✓	–	✓	–	294	ANN	PSO	Zhang et al. (2020)
✓	✓	✓	✓	–	✓	–	–	–	✓	–	385	RF	–	Zhang et al. (2021)
✓	✓	✓	✓	–	–	–	✓	–	✓	–	294	ANN, RF, SVM	PSO	Tang and Na (2021)
✓	✓	✓	✓	–	–	–	✓	–	✓	–	294	ANN	GA	Feng and Zhang (2022)
✓	✓	✓	–	–	–	–	–	–	✓	Surface surcharge	253	RF	–	Kim et al. (2022)
✓	✓	✓	✓	–	–	–	–	Deviation etc.	–	–	72	RF, MR	–	Ling et al. (2022)
✓	✓	✓	✓	–	–	–	–	–	–	–	65	ANN	PSO	Kong et al. (2022)

References

Afradi, A., Ebrahimabadi, A., Hallajian, T., 2019. Prediction of the penetration rate and number of consumed disc cutters of tunnel boring machines (TBMs) using artificial neural network (ANN) and support vector machine (SVM)-Case study: beheshtabad water conveyance tunnel in Iran. Asian J. Water Environ. Pollut. 16 (1), 49–57. https://doi.org/10.3233/AJW190006.

Ahangari, K., Moeinossadat, S.R., Behnia, D., 2015a. Estimation of tunnelling-induced settlement by modern intelligent methods. Soils Found. 55 (4), 737–748. https://doi.org/10.1016/j.sandf.2015.06.006.

Ahangari, K., Moeinossadat, S.R., Behnia, D., 2015b. Estimation of tunnelling-induced settlement by modern intelligent methods. Soils Found. 55 (4), 737–748. https://doi.org/10.1016/j.sandf.2015.06.006.

Ahmed, N.Z., El-Shourbagy, M., Akl, A., Metwally, K., 2021. Field monitoring and numerical analysis of ground deformation induced by tunnelling beneath an existing tunnel. Cogent Eng. 8 (1). https://doi.org/10.1080/23311916.2020.1861731.

Akbarzadeh, M., Shaffiee Haghshenas, S., Jalali, S.M.E., Zare, S., Mikaeil, R., 2022. Developing the rule of thumb for evaluating penetration rate of TBM, using binary classification. Geotech. Geol. Eng. 40 (9), 4685–4703. https://doi.org/10.1007/s10706-022-02178-7.

Antonio Bobet, B., 2001. Analytical solutions for shallow tunnels in 401 saturated ground.

Arioglu, E., 1992. Surface Movements Due to Tunnelling Activities in Urban Areas and Minimization of Building Damages.

Armaghani, D.J., He, B., Mohamad, E.T., Zhang, Y.X., Lai, S.H., Ye, F., 2023. Applications of two neuro-based metaheuristic techniques in evaluating ground vibration resulting from tunnel blasting. Mathematics 11 (1). https://doi.org/10.3390/math11010106.

Aswathy, M.S., Vinoth, M., Mittal, A., 2022. Impact of governing factors on prediction of tunneling induced surface settlement in Young alluvium deposit. Indian Geotech. J. 52 (1), 13–27. https://doi.org/10.1007/s40098-021-00561-4.

Attewell, P.B., Farmer, I.W., 1974. Ground deformations resulting from shield tunnelling in London clay. Can. Geotech. J. 380–395.

Attewell, P.B., P Woodman, J.P., 1982. Predicting the Dynamics of Ground Settlement and its Derivitives Caused by Tunnelling in Soil.

Attewell, P.B., Yeates, J., Selby, A.R., 1986. Soil Movement Induced by Tunnelling and Their Effects on Pipelines and Structures. London.

Bouayad, D., Emeriault, F., 2017. Modeling the relationship between ground surface settlements induced by shield tunneling and the operational and geological parameters based on the hybrid PCA/ANFIS method. Tunn. Undergr. Space Technol. 68, 142–152. https://doi.org/10.1016/j.tust.2017.03.011.

Chakeri, H., Balani, A., Sharghi, M., Özcelik, Y., 2021. An investigation into the effects of an annular gap on surface settlement. Soil Mech. Found. Eng. 57 (6), 506–512. https://doi.org/10.1007/s11204-021-09699-y.

Chakeri, H., Hasanpour, R., Hindistan, M.A., Ünver, B., 2011. Analysis of interaction between tunnels in soft ground by 3D numerical modeling. Bull. Eng. Geol. Environ. 70 (3), 439–448. https://doi.org/10.1007/s10064-010-0333-8.

Chakeri, H., Ozcelik, Y., Unver, B., 2013. Effects of important factors on surface settlement prediction for metro tunnel excavated by EPB. Tunn. Undergr. Space Technol. 36, 14–23. https://doi.org/10.1016/j.tust.2013.02.002.

Chakeri, H., Ünver, B., 2014. A new equation for estimating the maximum surface settlement above tunnels excavated in soft ground. Environ. Earth Sci. 71 (7), 3195–3210. https://doi.org/10.1007/s12665-013-2707-2.

Chen, J., Yang, T., Zhang, D., Huang, H., Tian, Y., 2021. Deep learning based classification of rock structure of tunnel face. Geosci. Front. 12 (1), 395–404. https://doi.org/10.1016/j.gsf.2020.04.003.

Chen, R.P., Zhang, P., Kang, X., Zhong, Z.Q., Liu, Y., Wu, H.N., 2019. Prediction of maximum surface settlement caused by earth pressure balance (EPB) shield tunneling with ANN methods. Soils Found. 59 (2), 284–295. https://doi.org/10.1016/j.sandf.2018.11.005.

Chen, R., Zhang, P., Wu, H., Wang, Z., Zhong, Z., 2019. Prediction of shield tunneling-induced ground settlement using machine learning techniques. Front. Struct. Civ. Eng. 13 (6), 1363–1378. https://doi.org/10.1007/s11709-019-0561-3.

Cheng, Y., Zhou, W.H., Xu, T., 2022. Tunneling-induced settlement prediction using the hybrid feature selection method for feature optimization. Trans. Geotech. 36. https://doi.org/10.1016/j.trgeo.2022.100808.

Cheng, Z.-L., Kannangara, K.K.P.M., Su, L.-J., Zhou, W.-H., 2023. Mathematical model for approximating shield tunneling-induced surface settlement via multi-gene genetic programming. Acta Geotechnica. https://doi.org/10.1007/s11440-023-01847-y.

Chi, S.-Y., Chern, J.-C., Lin, C.-C., 2001. Optimized back-analysis for tunneling-induced 455 ground movement using equivalent ground loss model. In Tunnelling and 456 Underground Space Technology (Vol. 16).

Chou, W.-I., Bobet, A., 2002. Predictions of ground deformations in shallow tunnels in clay. In: Tunnelling and Underground Space Technology, vol. 17.

Clough, G.W., Schmidt, B., 1981. In: Brand, E.W., Brenner, R.P. (Eds.), Design and Performance of Excavations and Tunnels in Soft Clay. Elsevier.

Darabi, A., Ahangari, K., Noorzad, A., Arab, A., 2012. Subsidence estimation utilizing various approaches - a case study: tehran No. 3 subway line. Tunn. Undergr. Space Technol. 31, 117–127. https://doi.org/10.1016/j.tust.2012.04.012.

Dehghan, A.N., Bagheri, E., Khodaei, M., Kalehsar, R.I., 2021. Evaluating the effect of EPBM operational parameters on surface settlement in soft ground. J. Geophys. Eng. 18 (1), 47–61. https://doi.org/10.1093/jge/gxaa067.

Deng, H., Liu, L., Fang, J., Qu, B., Huang, Q., 2023. A novel improved whale optimization algorithm for optimization problems with multi-strategy and hybrid algorithm. Math. Comput. Simulat. 205, 794–817. https://doi.org/10.1016/j.matcom.2022.10.023.

Deng, H.S., Fu, H.L., Yue, S., Huang, Z., Zhao, Y.Y., 2022. Ground loss model for analyzing shield tunneling-induced surface settlement along curve sections. Tunn. Undergr. Space Technol. 119. https://doi.org/10.1016/j.tust.2021.104250.

Deng, Z., Zhu, X., Cheng, D., Zong, M., Zhang, S., 2016. Efficient kNN classification algorithm for big data. Neurocomputing 195, 143–148. https://doi.org/10.1016/j.neucom.2015.08.112.

Ding, J., Zhang, S., Zhang, H., Guo, C., Liao, Z., Liu, H., 2021. Ground settlement caused by shield tunneling in soil-rock composite strata. J. Perform. Constr. Facil. 35 (5). https://doi.org/10.1061/(asce)cf.1943-5509.0001631.

Do, N.A., Dias, D., Golpasand, M.R.B., Dang, V.K., Nait-Rabah, O., Pham, V.V., Dang, T.T., 2022. Numerical analyses of twin stacked mechanized tunnels in soft grounds – influence of their position and construction procedure. Tunn. Undergr. Space Technol. 130. https://doi.org/10.1016/j.tust.2022.104734.

Do, N.A., Dias, D., Vu, T.T., Dang, V.K., 2021. Impact of the shield machine's performance parameters on the tunnel lining behaviour and settlements. Environ. Earth Sci. 80 (16). https://doi.org/10.1007/s12665-021-09820-2.

Do Ngoc, T., Van, K.D., Van, V.P., Van, Q.N., 2022. Prediction of surface settlement due to twin tunnel construction in soft ground of hanoi metro line 03. Int. J. GEOMATE 22 (94), 66–72. https://doi.org/10.21660/2022.94.3209.

Ercelebi, S.G., Copur, H., Bilgin, N., Feridunoglu, C., 2005. Underground space use : analysis of the past and lessons for the future : proceedings of the 31st ITA-AITES World Tunnel Congress. In: May 2005, Istanbul, Turkey. A.A. Balkema, pp. 7–12.

Ercelebi, S.G., Copur, H., Ocak, I., 2011. Surface settlement predictions for Istanbul Metro tunnels excavated by EPB-TBM. Environ. Earth Sci. 62 (2), 357–365. https://doi.org/10.1007/s12665-010-0530-6.

Fang, Y., He, C., Nazem, A., Yao, Z., Grasmick, J., 2017. Surface settlement prediction for EPB shield tunneling in sandy ground. KSCE J. Civ. Eng. 21 (7), 2908–2918. https://doi.org/10.1007/s12205-017-0989-8.

Fang, Q., Wang, G., Du, J., Liu, Y., Zhou, M., 2023. Prediction of tunnelling induced ground movement in clay using principle of minimum total potential energy. Tunnelling and Underground Space Technology 131. https://doi.org/10.1016/j.tust.2022.104854.

Fei, H., Tan, F., 2018. Bidirectional grid long short-term memory (BiGridLSTM): a method to address context-sensitivity and vanishing gradient. Algorithms 11 (11). https://doi.org/10.3390/a11110172.

Feng, L., Zhang, L., 2022. Enhanced prediction intervals of tunnel-induced settlement using the genetic algorithm and neural network. Reliab. Eng. Syst. Saf. 223. https://doi.org/10.1016/j.ress.2022.108439.

Feng, X., Wang, P., Liu, S., Wei, H., Miao, Y., Bu, S., 2022. Mechanism and law analysis on ground settlement caused by shield excavation of small-radius curved tunnel. Rock Mech. Rock Eng. 55 (6), 3473–3488. https://doi.org/10.1007/s00603-022-02819-6.

Franza, A., Marshall, A.M., 2019. Empirical and semi-analytical methods for evaluating 509 tunnelling-induced ground movements in sands. Tunnelling and Underground Space 510 Technology 88, 47–62. https://doi.org/10.1016/j.tust.2019.02.016.

Ge, S., Gao, W., Cui, S., Chen, X., Wang, S., 2022. Safety prediction of shield tunnel construction using deep belief network and whale optimization algorithm. Automation in Construction 142. https://doi.org/10.1016/j.autcon.2022.104488.

Ghiasi, V., Koushki, M., 2020. Numerical and artificial neural network analyses of ground surface settlement of tunnel in saturated soil. SN Appl. Sci. 2 (5). https://doi.org/10.1007/s42452-020-2742-z.

Glossop, N.H., 1978. Soil Deformation Caused by Soft Ground Tunneling. University of Durham.

Goh, A.T.C., Zhang, W., Zhang, Y., Xiao, Y., Xiang, Y., 2018. Determination of earth pressure balance tunnel-related maximum surface settlement: a multivariate adaptive regression splines approach. Bull. Eng. Geol. Environ. 77 (2), 489–500. https://doi.org/10.1007/s10064-016-0937-8.

Gonzaíez, C., Sagaseta, C., 2001. Patterns of soil deformations around tunnels. 524 Application to the extension of Madrid Metro.

Hage Chehade, F., Shahrour, I., 2008. Numerical analysis of the interaction between twin-tunnels: influence of the relative position and construction procedure. Tunn. Undergr. Space Technol. 23 (2), 210–214. https://doi.org/10.1016/j.tust.2007.03.004.

Hajihassani, M., Jahed Armaghani, D., Kalatehjari, R., 2018. Applications of particle swarm optimization in geotechnical engineering: a comprehensive review. In: Geotechnical and Geological Engineering, vol. 36. Springer International Publishing, pp. 705–722. https://doi.org/10.1007/s10706-017-0356-z.

Hajihassani, M., Kalatehjari, R., Marto, A., Mohamad, H., Khosrotash, M., 2020. 3D prediction of tunneling-induced ground movements based on a hybrid ANN and empirical methods. Eng. Comput. 36 (1), 251–269. https://doi.org/10.1007/s00366-018-00699-5.

Hamza, M., Ata, A., Roussin, A., 1999. Ground movements due to construction of cut and cover structures and slurry shield tunnel of the Cairo metro. Tunn. Undergr. Space Technol. 281–289.

Hao, D., Zhu, R., Wu, K., Chen, R., 2022. Analysis of ground settlement caused by double-line TBM tunnelling under existing building. Geotech. Geol. Eng. 40 (2), 899–911. https://doi.org/10.1007/s10706-021-01934-5.

Hasanipanah, M., Noorian-Bidgoli, M., Jahed Armaghani, D., Khamesi, H., 2016. Feasibility of PSO-ANN model for predicting surface settlement caused by tunneling. Eng. Comput. 32 (4), 705–715. https://doi.org/10.1007/s00366-016-0447-0.

Hasanpour, R., Chakeri, H., Ozcelik, Y., Denek, H., 2012. Evaluation of surface settlements in the Istanbul metro in terms of analytical, numerical and direct measurements. Bull. Eng. Geol. Environ. 71 (3), 499–510. https://doi.org/10.1007/s10064-012-0428-5.

He, S., Li, C., Wang, D., Liu, X., 2021. Surface settlement induced by slurry shield tunnelling in sandy cobble strata—a case study. Indian Geotech. J. 51 (6), 1349–1363. https://doi.org/10.1007/s40098-021-00543-6.

Herzog, M., 1985. Surface subsidence above shallow tunnels. Bautechnik 62, 375–377.

Hosseini, S., Al Khaled, A., 2014. A survey on the Imperialist Competitive Algorithm metaheuristic: implementation in engineering domain and directions for future research. In: Applied Soft Computing, vol. 24. Elsevier Ltd, pp. 1078–1094. https://doi.org/10.1016/j.asoc.2014.08.024.
Hou, Y., Zhou, M., Zhang, D., Fang, Q., Sun, Z., Tian, Y., 2022. Analysis of four shield-driven tunnels with complex spatial relations in a clay stratum. Tunn. Undergr. Space Technol. 124. https://doi.org/10.1016/j.tust.2022.104478.
Houhou, M.N., Amari, T., Belounar, A., 2022. Three-dimensional numerical analyses of pile responses to tunneling-induced ground movements in bilayer soil. World J. Eng. https://doi.org/10.1108/WJE-04-2022-0159.
Hu, Y., Lei, H., Zheng, G., Shi, L., Zhang, T., Shen, Z., Jia, R., 2022. Ground movement induced by triple stacked tunneling with different construction sequences. J. Rock Mech. Geotech. Eng. 14 (5), 1433–1446. https://doi.org/10.1016/j.jrmge.2022.03.003.
Huang, H., Gong, W., Khoshnevisan, S., Juang, C.H., Zhang, D., Wang, L., 2015. Simplified procedure for finite element analysis of the longitudinal performance of shield tunnels considering spatial soil variability in longitudinal direction. Comput. Geotech. 64, 132–145. https://doi.org/10.1016/j.compgeo.2014.11.010.
Huang, H.W., Xiao, L., Zhang, D.M., Zhang, J., 2017. Influence of spatial variability of soil Young's modulus on tunnel convergence in soft soils. Eng. Geol. 228, 357–370. https://doi.org/10.1016/j.enggeo.2017.09.011.
Idinger, G., Aklik, P., Wu, W., Borja, R.I., 2011. Centrifuge model test on the face stability of shallow tunnel. Acta Geotechnica 6 (2), 105–117. https://doi.org/10.1007/s11440-011-0139-2.
Kannangara, K.K.P.M., Zhou, W., Ding, Z., Hong, Z., 2022. Investigation of feature contribution to shield tunneling-induced settlement using Shapley additive explanations method. J. Rock Mech. Geotech. Eng. 14 (4), 1052–1063. https://doi.org/10.1016/j.jrmge.2022.01.002.
Karakus, M., 2007. Appraising the methods accounting for 3D tunnelling effects in 2D plane strain FE analysis. Tunn. Undergr. Space Technol. 22 (1), 47–56. https://doi.org/10.1016/j.tust.2006.01.004.
Kasper, T., Meschke, G., 2004. A 3D finite element simulation model for TBM tunnelling in soft ground. Int. J. Numer. Anal. Methods GeoMech. 28 (14), 1441–1460. https://doi.org/10.1002/nag.395.
Kasper, T., Meschke, G., 2006a. A numerical study of the effect of soil and grout material properties and cover depth in shield tunnelling. Comput. Geotech. 33 (4–5), 234–247. https://doi.org/10.1016/j.compgeo.2006.04.004.
Kasper, T., Meschke, G., 2006b. On the influence of face pressure, grouting pressure and TBM design in soft ground tunnelling. Tunn. Undergr. Space Technol. 21 (2), 160–171. https://doi.org/10.1016/j.tust.2005.06.006.
Ke, W., zheng, Z., Shuchen, L., leisheng, Z., Jiahui, Z., Yang, Z., 2021. Mechanical aspects of construction of new TBM tunnel under existing structures. Geotech. Geol. Eng. 39 (8), 5727–5741. https://doi.org/10.1007/s10706-021-01860-6.
Kim, C. Y., Bae, G. J., Hong, S. W., Park, C. H., Moon, H. K., Shin, H. S., 2001. Neural 587 network based prediction of ground surface settlements due to tunnelling. 588.
Kim, D., Pham, K., Oh, J.Y., Lee, S.J., Choi, H., 2022. Classification of surface settlement levels induced by TBM driving in urban areas using random forest with data-driven feature selection. Automation in Construction 135. https://doi.org/10.1016/j.autcon.2021.104109.
Kingsford, C., Salzberg, S.L., 2022. What are decision trees? Nature Biotechnology 26. http://www.nature.com/naturebiotechnology, 2008.
Kong, F., Lu, D., Ma, Y., Li, J., Tian, T., 2022. Analysis and Intelligent Prediction for Displacement of Stratum and Tunnel Lining by Shield Tunnel Excavation in Complex Geological Conditions: A Case Study. IEEE Transactions on Intelligent Transportation Systems 23 (11), 22206–22216. https://doi.org/10.1109/TITS.2022.3149819.
Kong, F.C., Lu, D.C., Ma, Y.D., Tian, T., Yu, H.T., Du, X.L., 2022. Novel hybrid method to predict the ground-displacement field caused by shallow tunnel excavation. Science China Technological Sciences 66 (1), 101–114. https://doi.org/10.1007/s11431-022-2079-8.
Kotsiantis, S.B., 2013. Decision trees: a recent overview. In: Artificial Intelligence Review, vol. 39, pp. 261–283. https://doi.org/10.1007/s10462-011-9272-4.
Krishna, G., Maji, V.B., 2022. Numerical simulation of EPBM induced ground settlement. Indian Geotech. J. 52 (2), 341–351. https://doi.org/10.1007/s40098-021-00568-x.
Lee, C.-J., 1999. Soil Movements Around a Tunnel in Soft Soils Earthquake-Induced Permanent Settlement of Shallow Foundation of Bridges Rested on Liquefiable Sand: Centrifuge and Numerical Modeling View Project. https://www.researchgate.net/publication/255660738.
Li, M., Du, W., Nian, F., 2014. An adaptive particle swarm optimization algorithm based on directed weighted complex network. Math. Probl Eng. https://doi.org/10.1155/2014/434972, 2014.
Li, R., Lei, H., Liu, Y., Zhang, Y., Hu, Y., 2022. Ground movement and existing tunnel deformation induced by overlapped tunneling. Int. J. GeoMech. 22 (7). https://doi.org/10.1061/(asce)gm.1943-5622.0002431.
Li, S., hua, Zhang, ju, M., Li, P. fei, 2021. Analytical solutions to ground settlement induced by ground loss and construction loadings during curved shield tunneling. J. Zhejiang Univ. - Sci. 22 (4), 296–313. https://doi.org/10.1631/jzus.A2000120.
Li, S., Zhang, Y., Cao, M., Wang, Z., 2022. Study on excavation sequence of pilot tunnels for a rectangular tunnel using numerical simulation and field monitoring method. Rock Mech. Rock Eng. 55 (6), 3507–3523. https://doi.org/10.1007/s00603-022-02814-x.
Ling, X., Kong, X., Tang, L., Zhao, Y., Tang, W., Zhang, Y., 2022. Predicting earth pressure balance (EPB) shield tunneling-induced ground settlement in compound strata using random forest. Transportation Geotechnics 35. https://doi.org/10.1016/j.trgeo.2022.100771.
Liu, L., Zhou, W., Gutierrez, M., 2022. Effectiveness of predicting tunneling-induced ground settlements using machine learning methods with small datasets. J. Rock Mech. Geotech. Eng. 14 (4), 1028–1041. https://doi.org/10.1016/j.jrmge.2021.08.018.
Loganathan, N., Poulos, H.G., Stewart, D.P., 2000. Centrifuge model testing of tunnelling-induced ground and pile deformations. Geotechnique.
Loganathan, B.N., Poulos, H.G., 1998. Analytical prediction for tunneling-induced ground movements in clays.
Ma, S., Li, J., Li, Z., 2022. Critical support pressure of shield tunnel face in soft-hard mixed strata. Trans. Geotech. 37. https://doi.org/10.1016/j.trgeo.2022.100853.
Mahdevari, S., Torabi, S.R., Monjezi, M., 2012. Application of artificial intelligence algorithms in predicting tunnel convergence to avoid TBM jamming phenomenon. Int. J. Rock Mech. Min. Sci. 55, 33–44. https://doi.org/10.1016/j.ijrmms.2012.06.005.
Mahmoodzadeh, A., Mohammadi, M., Daraei, A., Farid Hama Ali, H., Kameran Al-Salihi, N., Mohammed Dler Omer, R., 2020. Forecasting maximum surface settlement caused by urban tunneling. Automation in Construction 120. https://doi.org/10.1016/j.autcon.2020.103375.
Mahmoodzadeh, A., Mohammadi, M., Farid Hama Ali, H., Hashim Ibrahim, H., Nariman Abdulhamid, S., Nejati, H.R., 2022. Prediction of safety factors for slope stability: comparison of machine learning techniques. Nat. Hazards 111 (2), 1771–1799. https://doi.org/10.1007/s11069-021-05115-8.
Mair, R.J., Taylor, R.N., 1997. Bored tunnelling in the urban environment. In: 14th Int. Conf. On Soil Mechanics and Foundation Engineering, pp. 2353–2385.
Mair, R.J., Taylor, R.N., Bracegirdle, A., 1993. Subsurface settlement profiles above tunnels in clays. Geotechnique 315–320.
Mansour, M.F., El-Nahhas, F.M., Elshanawany, A.M., 2021. Short and long-term behaviours of bored tunnels in port-said clay. Geotech. Geol. Eng. 39 (6), 4563–4580. https://doi.org/10.1007/s10706-021-01784-1.
Martos, F., 1958. Concerning an approximate equation of the subsidence trough and its time factor. Int. Strata Control Cong. 191–205.
Meharie, M.G., Shaik, N., 2020. Predicting highway construction costs: comparison of the performance of random forest, neural network and support vector machine models. J. Soft Comput. Civil Eng. 4 (2), 103–112. https://doi.org/10.22115/SCCE.2020.226883.1205.
Miao, J.B., Lu, D.C., Lin, Q.T., Kong, F.C., Du, X.L., 2021. Time-dependent surrounding soil pressure and mechanical response of tunnel lining induced by surrounding soil viscosity. Sci. China Technol. Sci. 64 (11), 2453–2468. https://doi.org/10.1007/s11431-021-1908-6.
Moeinossadat, S.R., Ahangari, K., Shahriar, K., 2018. Modeling maximum surface settlement due to EPBM tunneling by various soft computing techniques. Innovative Infrastructure Solutions 3 (1). https://doi.org/10.1007/s41062-017-0114-3.
Moghaddasi, M.R., Noorian-Bidgoli, M., 2018. ICA-ANN, ANN and multiple regression models for prediction of surface settlement caused by tunneling. Tunn. Undergr. Space Technol. 79, 197–209. https://doi.org/10.1016/j.tust.2018.04.016.
Mohammadi, H., Azad, A., 2021. Prediction of ground settlement and the corresponding risk induced by tunneling: an application of rock engineering system paradigm. Tunn. Undergr. Space Technol. 110. https://doi.org/10.1016/j.tust.2021.103828.
Mohammadi, S.D., Naseri, F., Alipoor, S., 2015. Development of artificial neural networks and multiple regression models for the NATM tunnelling-induced settlement in Niayesh subway tunnel, Tehran. Bulletin of Engineering Geology and the Environment 74 (3), 827–843. https://doi.org/10.1007/s10064-014-0660-2.
Mojtahedi, A.S., Nabizadeh, A., 2022. A numerical approach to evaluating the asymmetric ground settlement response to twin-tunnel asynchronous excavation. Soils and Rocks 45 (2). https://doi.org/10.28927/SR.2022.071021.
Mroueh, H., Shahrour, I., 2003. A full 3-D finite element analysis of tunneling-adjacent structures interaction. Comput. Geotech. 30 (3), 245–253. https://doi.org/10.1016/S0266-352X(02)00047-2.
Mu, B., Xie, X., Li, X., Li, J., Shao, C., Zhao, J., 2021. Monitoring, modelling and prediction of segmental lining deformation and ground settlement of an EPB tunnel in different soils. Tunn. Undergr. Space Technol. 113. https://doi.org/10.1016/j.tust.2021.103870.
Navada, A., Ansari, A.N., Patil, S., Sonkamble, B.A., 2011. Overview of use of decision tree algorithms in machine learning. In: Proceedings - 2011 IEEE Control and System Graduate Research Colloquium. ICSGRC, pp. 37–42. https://doi.org/10.1109/ICSGRC.2011.5991826, 2011.
New, B.M., O'Reilly, M.P., 1991. Tunnelling induced ground movements: Predicting 695 their magnitude and effects. In: 4th Int. Conf. on Ground Movements and Structures, 671– 696 697.
Ocak, I., Seker, S.E., 2013. Calculation of surface settlements caused by EPBM tunneling using artificial neural network, SVM, and Gaussian processes. Environ. Earth Sci. 70 (3), 1263–1276. https://doi.org/10.1007/s12665-012-2214-x.
O'Reilly, M.P., New, B.M., 1982. Settlements above tunnels in the United Kingdom-Their magnitude and prediction. In: Proc., 3rd Int. Symp., Institute of Mining and Metallurgy, London, pp. 173–181.
Pan, Y., Zhang, L., 2022. Mitigating tunnel-induced damages using deep neural networks. Automation in Construction 138. https://doi.org/10.1016/j.autcon.2022.104219.
Park, K.H., 2004. Elastic solution for tunneling-induced ground movements in clays. Int. J. GeoMech. 4 (4), 310–318.
Peck, R.B., 1969. Deep excavations and tunneling in soft ground. In: Proceedings of the 7th International Conference on Soil Mechanics and Foundation Engineering, pp. 225–290.
Pirastehfar, K., Shivaei, S., Sadaghiani, M.H., Nikooee, E., 2022. 3D numerical investigation of the effects of driving of the new mechanized tunnel on existing segmental linings and ground surface settlements - a case study: shiraz metro line 2. Int. J. Geotech. Eng. 16 (7), 878–889. https://doi.org/10.1080/19386362.2020.1816381.

Podgorelec, V., Kokol, P., Stiglic, B., Rozman, I., 2002. Decision trees: an overview and their use in medicine. J. Med. Syst. 26 (Issue 5).
Potts, D.M., 1997. A structure's influence on tunnelling-induced ground movements. Geotech. Eng. 109–125.
Pourtaghi, A., Lotfollahi-Yaghin, M.A., 2012. Wavenet ability assessment in comparison to ANN for predicting the maximum surface settlement caused by tunneling. Tunn. Undergr. Space Technol. 28 (1), 257–271. https://doi.org/10.1016/j.tust.2011.11.008.
Quinlan, J.R., 1990. Decision trees and decisionmaking. IEEE Trans. Syst., Man Cybern. 20 (2), 339–346. https://doi.org/10.1109/21.52545.
Ranken, W.J., 1987. Ground movement resulting from urban tunnelling: predictions and effects. Eng. Geol. Underground Movem. 79–92.
Saeed, H., Uygar, E., 2022. Equation for maximum ground surface settlement due to bored tunnelling in cohesive and cohesionless soils obtained by numerical simulations. Arabian J. Sci. Eng. 47 (4), 5139–5165. https://doi.org/10.1007/s13369-021-06436-3.
Sagaseta, C., 1987. Analysis of undrained soil deformation due to ground loss, 37 (Issue 3).
Schmidt, B., 1969. A method of estimating surface settlement above tunnels constructed in soft ground. Can. Geotech. J. 11–22.
Shen, S.L., Wu, H.N., Cui, Y.J., Yin, Z.Y., 2014. Long-term settlement behaviour of metro tunnels in the soft deposits of Shanghai. Tunn. Undergr. Space Technol. 40, 309–323. https://doi.org/10.1016/j.tust.2013.10.013.
Sherstinsky, A., 2020. Fundamentals of recurrent neural network (RNN) and long short-term memory (LSTM) network. Phys. Nonlinear Phenom. 404. https://doi.org/10.1016/j.physd.2019.132306.
Su, J., Wang, Y., Niu, X., Sha, S., Yu, J., 2022. Prediction of Ground Surface Settlement by Shield Tunneling Using XGBoost and Bayesian Optimization, vol. 114. Engineering Applications of Artificial Intelligence. https://doi.org/10.1016/j.engappai.2022.105020.
Suwansawat, S., Einstein, H.H., 2006. Artificial neural networks for predicting the maximum surface settlement caused by EPB shield tunneling. Tunn. Undergr. Space Technol. 21 (2), 133–150. https://doi.org/10.1016/j.tust.2005.06.007.
Swain, P.H., Hauska, H., 1977. Decision tree classifier: design and potential. IEEE Trans. Geosci. Electron., GE- 15 (3), 142–147. https://doi.org/10.1109/tge.1977.6498972.
Tang, L., Na, S.H., 2021. Comparison of machine learning methods for ground settlement prediction with different tunneling datasets. J. Rock Mech. Geotech. Eng. 13 (6), 1274–1289. https://doi.org/10.1016/j.jrmge.2021.08.006.
Tian, Y., Lu, D., Yao, Y., Du, X., Gao, Y., 2022. Formula of passive earth pressure and prediction of tunneling-induced settlement in anisotropic ground based on a simple method. Int. J. GeoMech. 22 (10). https://doi.org/10.1061/(asce)gm.1943-5622.0002573.
Topal, C., Mahmutoğlu, Y., 2021. Assessment of surface settlement induced by tunnel excavations for the esenler–başakşehir (istanbul, Turkey) subway line. Environ. Earth Sci. 80 (5). https://doi.org/10.1007/s12665-021-09509-6.
Verruijt, A., Booker, J.R., 1996. Surface settlements due to deformation of a tunnel in 759 an elastic half plane.
Vitali, O.P.M., Celestino, T.B., Bobet, A., 2022. Construction strategies for a NATM tunnel in São Paulo, Brazil, in residual soil. Undergr. Space 7 (1), 1–18. https://doi.org/10.1016/j.undsp.2021.04.002.
Wang, F., 2021. Empirical evidence for estimation of subsurface settlement caused by tunneling in sand. Undergr. Space 6 (5), 577–584. https://doi.org/10.1016/j.undsp.2021.01.002.
Wang, F., Du, X., Li, P., 2023. Predictions of ground surface settlement for shield tunnels in sandy cobble stratum based on stochastic medium theory and empirical formulas. Undergr. Space 11, 189–203. https://doi.org/10.1016/j.undsp.2023.01.003.
Wang, F., Gou, B., Qin, Y., 2013. Modeling tunneling-induced ground surface settlement development using a wavelet smooth relevance vector machine. Comput. Geotech. 54, 125–132. https://doi.org/10.1016/j.compgeo.2013.07.004.
Wang, F., Miao, L., Yang, X., Du, Y.J., Liang, F.Y., 2016. The volume of settlement trough change with depth caused by tunneling in sands. KSCE J. Civ. Eng. 20 (7), 2719–2724. https://doi.org/10.1007/s12205-016-0250-x.
Wang, Z.Z., Xiao, C., Goh, S.H., Deng, M.-X., 2021. Metamodel-based reliability analysis in spatially variable soils using convolutional neural networks. J. Geotech. Geoenviron. Eng. 147 (3). https://doi.org/10.1061/(asce)gt.1943-5606.0002486.
Wu, H.N., Shen, S.L., Liao, S.M., Yin, Z.Y., 2015. Longitudinal structural modelling of shield tunnels considering shearing dislocation between segmental rings. Tunn. Undergr. Space Technol. 50, 317–323. https://doi.org/10.1016/j.tust.2015.08.001.
Xie, X., Yang, Y., Ji, M., 2016. Analysis of ground surface settlement induced by the construction of a large-diameter shield-driven tunnel in Shanghai, China. Tunn. Undergr. Space Technol. 51, 120–132. https://doi.org/10.1016/j.tust.2015.10.008.
Xu, Q., Zhang, M., Gu, Z., Pan, G., 2019. Overfitting remedy by sparsifying regularization on fully-connected layers of CNNs. Neurocomputing 328, 69–74. https://doi.org/10.1016/j.neucom.2018.03.080.
Yoshikoshi, W., Osamu, W., Takagaki, N., 1978. Prediction of Ground Settlements Associated with Shield Tunneling. Soils Found, pp. 47–59.
Yuan, W., Fu, H., Zhang, J., Huang, Z., 2018. Analytical prediction for tunneling-induced ground movements with modified deformation pattern. Int. J. GeoMech. 18 (6). https://doi.org/10.1061/(asce)gm.1943-5622.0001156.
Zhang, J., Phoon, K.K., Zhang, D., Huang, H., Tang, C., 2021a. Deep learning-based evaluation of factor of safety with confidence interval for tunnel deformation in spatially variable soil. J. Rock Mech. Geotech. Eng. 13 (6), 1358–1367. https://doi.org/10.1016/j.jrmge.2021.09.001.
Zhang, J., Phoon, K.K., Zhang, D., Huang, H., Tang, C., 2021b. Deep learning-based evaluation of factor of safety with confidence interval for tunnel deformation in spatially variable soil. J. Rock Mech. Geotech. Eng. 13 (6), 1358–1367. https://doi.org/10.1016/j.jrmge.2021.09.001.
Zhang, J.Z., Huang, H.W., Zhang, D.M., Zhou, M.L., Tang, C., Liu, D.J., 2021. Effect of ground surface surcharge on deformational performance of tunnel in spatially variable soil. Comput. Geotech. 136. https://doi.org/10.1016/j.compgeo.2021.104229.
Zhang, L., Wu, X., Ji, W., AbouRizk, S.M., 2017. Intelligent approach to estimation of tunnel-induced ground settlement using wavelet packet and support vector machines. J. Comput. Civ. Eng. 31 (2). https://doi.org/10.1061/(asce)cp.1943-5487.0000621.
Zhang, P., 2019. A novel feature selection method based on global sensitivity analysis with application in machine learning-based prediction model. Appl. Soft Comput. J. 85. https://doi.org/10.1016/j.asoc.2019.105859.
Zhang, P., Wu, H.N., Chen, R.P., Chan, T.H.T., 2020. Hybrid meta-heuristic and machine learning algorithms for tunneling-induced settlement prediction: a comparative study. Tunn. Undergr. Space Technol. 99. https://doi.org/10.1016/j.tust.2020.103383.
Zhang, P., Yin, Z.-Y., Chen, R.-P., 2020. Analytical and semi-analytical solutions for describing tunneling-induced transverse and longitudinal settlement troughs. Int. J. GeoMech. 20 (8). https://doi.org/10.1061/(asce)gm.1943-5622.0001748.
Zhang, Q., Zhang, X.P., Wang, H.J., Liu, Q.S., Xu, D., Tang, S.H., 2022. Numerical study of the effect of grout material properties on ground deformation during shallow TBM tunneling. KSCE J. Civ. Eng. 26 (8), 3590–3599. https://doi.org/10.1007/s12205-022-1028-y.
Zhang, S., Li, X., Zong, M., Zhu, X., Cheng, D., 2017. Learning k for kNN Classification. ACM Trans. Intell. Syst. Technol. 8 (3). https://doi.org/10.1145/2990508.
Zhang, L., Wu, X., Liu, W., Skibniewski, M.J., 2019. Optimal Strategy to Mitigate Tunnel-Induced Settlement in Soft Soils: Simulation Approach. J. Perform. Constructed Facilities 33 (5). https://doi.org/10.1061/(asce)cf.1943-5509.0001322.
Zhang, P., Chen, R.P., Wu, H.N., 2019. Real-time analysis and regulation of EPB shield steering using Random Forest. *Automation in Construction*, p. 106. https://doi.org/10.1016/j.autcon.2019.102860.
Zhang, W.G., Goh, A.T.C., 2013. Multivariate adaptive regression splines for analysis of geotechnical engineering systems. Computers and Geotechnics 48, 82–95. https://doi.org/10.1016/j.compgeo.2012.09.016.
Zhang, Z., Huang, M., Zhang, C., Jiang, K., Bai, Q., 2020. Analytical prediction of tunneling-induced ground movements and liner deformation in saturated soils considering influences of shield air pressure. Appl. Math. Model. 78, 749–772. https://doi.org/10.1016/j.apm.2019.10.025.
Zhao, C., Alimardani Lavasan, A., Barciaga, T., Kämper, C., Mark, P., Schanz, T., 2017. Prediction of tunnel lining forces and deformations using analytical and numerical solutions. Tunn. Undergr. Space Technol. 64, 164–176. https://doi.org/10.1016/j.tust.2017.01.015.
Zhao, C., Mahmoudi, E., Luo, M., Jiang, M., Lin, P., 2023. Unfavorable geology recognition in front of shallow tunnel face using machine learning. Comput. Geotech. 157. https://doi.org/10.1016/j.compgeo.2023.105313.
Zheng, G., Fan, Q., Zhang, T., Zhang, Q., 2022. Numerical study of the Soil-Tunnel and Tunnel-Tunnel interactions of EPBM overlapping tunnels constructed in soft ground. Tunn. Undergr. Space Technol. 124. https://doi.org/10.1016/j.tust.2022.104490.
Zhong, Z., Li, C., Liu, X., Fan, Y., Liang, N., 2021. Analysis of ground surface settlement induced by the construction of mechanized twin tunnels in soil-rock mass mixed ground. Tunn. Undergr. Space Technol. 110. https://doi.org/10.1016/j.tust.2020.103746.
Zhou, J., Shi, Xiuzhi, Du, Kun, Xianyang Qiu, Li, X., Mitri, H.S., 2016. Feasibility of Random-Forest Approach for Prediction of Ground Settlements Induced by the Construction of a Shield-Driven Tunnel. https://doi.org/10.1061/(ASCE.
Zhu, C., Wang, S., Peng, S., Song, Y., 2022. Surface settlement in saturated loess stratum during shield construction: numerical modeling and sensitivity analysis. Tunn. Undergr. Space Technol. 119. https://doi.org/10.1016/j.tust.2021.104205.